Roll Bonding Processes: State-of-the-Art and Future Perspectives

Haris Ali Khan [1,*], Kamran Asim [1], Farooq Akram [1] [iD], Asad Hameed [1], Abdullah Khan [2] and Bilal Mansoor [3,4,*]

[1] Aerospace Engineering Department, College of Aeronautical Engineering, National University of Sciences and Technology (NUST), H-12, Islamabad 44000, Pakistan; kamran@cae.nust.edu.pk (K.A.); farooq@cae.nust.edu.pk (F.A.); asadhameed@cae.nust.edu.pk (A.H.)

[2] Morgan Advanced Materials, 310 Innovation Blvd, State College, PA 16803, USA; Abdullah.Khan@morganplc.com

[3] Mechanical Engineering Program, Texas A&M University at Qatar, Education City, Doha P.O. Box 23874, Qatar

[4] Department of Materials Science and Engineering, Texas A&M University, 3003 TAMU, College Station, TX 77843, USA

[*] Correspondence: hakhan@cae.nust.edu.pk (H.A.K.); bilal.mansoor@tamu.edu (B.M.); Tel.: +974-4423-0240 (B.M.)

Abstract: Roll bonding (RB) describes solid-state manufacturing processes where cold or hot rolling of plates or sheet metal is carried out for joining similar and dissimilar materials through the principle of severe plastic deformation. This review covers the mechanics of RB processes, identifies the key process parameters, and provides a detailed discussion on their scientific and/or engineering aspects, which influence the microstructure–mechanical behavior relations of processed materials. It further evaluates the available research focused on improving the metallurgical and mechanical behavior of bonded materials such as microstructure modification, strength enhancement, local mechanical properties, and corrosion and electrical resistance evolution. Moreover, current applications and advantages, limitations of the process and developments in dissimilar material hot roll bonding technologies for producing titanium to steel and stainless steel to carbon steel ultra-thick plates are also discussed. The paper concludes by deliberating on the bonding mechanisms, engineering guidelines and process–property–structure relationships, and recommending probable areas for future research.

1. Introduction

Nearly all engineering structures are an assemblage of several distinct components that require the application of a joining process. The selection of a certain joining technique plays a key part in determining the overall service life and functionality of an engineering structure in a particular environment. On the other hand, the key engineering elements in the selection of a joining process include materials to be joined, function, mode of loading and joint geometry and physical attributes, such as component topology, profile, accessibility, section thickness and tolerance. In addition, the desired functional requirements and ease of maintenance, which in turn depend on weld quality, i.e., microstructure and properties (mechanical, electrical, etc.), also dictate the choice of process selection. For instance, in light-metal transportation structures exposed to a range of different environments, joining processes such as riveting are preferred compared to fusion welding processes to avoid the detrimental effects of melting leading to degradation of mechanical properties. In a similar vein, there are many other applications, particularly those which involve the joining of dissimilar materials, where conventional fusion welding processes are rendered infeasible, and hence solid-state joining processes are attractive.

In solid-state joining processes, true metallurgical welds are obtained without melting—although some local and isolated pockets of melting may form—thus, bulk volume changes caused by solidification are avoided during the process [1]. In the last few decades, several solid-state joining and manufacturing processes have gained noticeable attention, owing to the inherent advantages of this technology. Several processes and variants, including friction stir welding [2], friction stir riveting [3], ultrasonic welding [4], roll bonding [5], etc., are considered to be quite mature and have been extensively used by industry for decades now. These processes can be used to induce desired changes at the microstructural level and to form bonds between metallic sheets of similar and dissimilar materials [6]. Solid-state methods therefore provide a wide range of joining solutions considering the functional requirements and component topology. Therefore, advancing solid-state joining processes remains an ongoing technical and scientific goal among the joining research community. As a result, these processes are constantly being looked at for further development, as is evident from the six-fold increase in research citations related to solid-state joining processes during the last decade.

In this context, two functional requirements that have attracted increasing attention in the last few years include: (1) the ability to join dissimilar metals that cannot be welded by conventional processes, such as joining stainless steel or steel to nickel, titanium, copper, and aluminum alloys, (2) the development of thick or ultra-thick layered composite materials with potential applications ranging from simple bi-metal strips for engine components to complex turbine blades as functional gradient structures. Different solid-state joining processes have been employed for the manufacturing such structures. The roll bonding process, among them, have shown significant potential and can be classified among the solid-state processes in which extensive mechanical deformation is produced in a metallic sheet with or without application of heat to change the microstructure or to create bonds between multiple metal sheets [7]. For example, cold roll bonding is a mature technology typically deployed to produce roll-clad plates to protect against corrosion or erosive wear encountered in various important industries. Some of the advantages of the RB process over conventional manufacturing and joining processes include simplicity and ease of operation, cost savings, desirable mechanical properties, and applicability to dissimilar materials. A detailed literature review indicates that a diversity of research is available on RB processes, including development and optimization process parameters, evolution of microstructure and mechanical properties for different materials and configurations. In addition, several review papers on different variants of the RB process are also available, providing comprehensive coverage of the research performed. However, to fully exploit any process, a thorough understanding of the relationship between processing parameters and the resultant performance indicators (i.e., mechanical, and electrical properties, behavior under hostile environment) is mandatory. Unfortunately, such a requirement has not been explicitly addressed in previous reviews. Moreover, no review paper is available that provides a comparative analysis of the different variants of the RB process. Such an analysis can help the designer to carefully select the process according to the requisite applications.

This review paper is, therefore, aims to serve as the missing link that can interconnect key aspects such as process parameters, microstructure, and defects, and their influence on the resultant properties. Moreover, a detailed discussion on the major variants of the RB processes (i.e., cold roll bonding, hot roll bonding, and accumulative roll bonding) is presented in this paper to provide a comparison of the different variants of the RB process. The paper covers different aspects of the RB process, including process mechanics, characterization, and evaluation (mechanical, electrical, and extreme environment), and modeling. An effort is made to discuss current applications and advantages, the limitations of the process, and developments in dissimilar material hot roll bonding technologies. For each aspect, research needs are identified and presented at the end of the respective section. The paper concludes by presenting some critical analyses, including joining mechanisms, engineering guidelines, and process–structure–property relationships. Finally, future research areas are identified based on modern manufacturing trends.

2. Process Description

2.1. Introduction

The roll bonding (RB) process involves the joining of two or more sheets of similar or dissimilar materials at various temperatures. The process requires rolling through a pair of rollers under adequate pressure resulting in the bonding of sheets [8]. The process is categorized into three types, i.e., cold, hot, and warm roll bonding based on the ranges of the processing temperature which in turn is related to the recrystallization temperature [9].

2.2. Process Variants

The variants in the RB process primarily originate from the difference in processing temperatures. A brief description of these methods is provided in the following paragraphs.

2.2.1. Cold Roll Bonding (CRB) Process

The CRB process is defined by the processing temperature being less than the recrystallization temperature [10]. Figure 1 describes the steps involved in the process. The first step in the process is the stacking of sheets, plates, or foils, after which a pair of rollers are passed over them in the next stage. The rolling process is continued until the deformation required to achieve solid-state bonding among the parent materials is obtained [11,12]. The parent materials experience substantial reduction to reach the threshold to achieve bonding during the process under high pressure exerted by the rollers [13]. This threshold reduction results in the generation of a significant amount of heat, which subsequently produces a bond through asperity contact and atomic affinity between the two sheets. CRB is also known as cold pressure welding by rolling [14,15], clad sheet by rolling [16–18]. A variety of materials, either similar or dissimilar, can be joined through CRB [19,20]. A review by Jamaati et al. covered the strength aspect of joints fabricated by cold roll bonding in great detail [17].
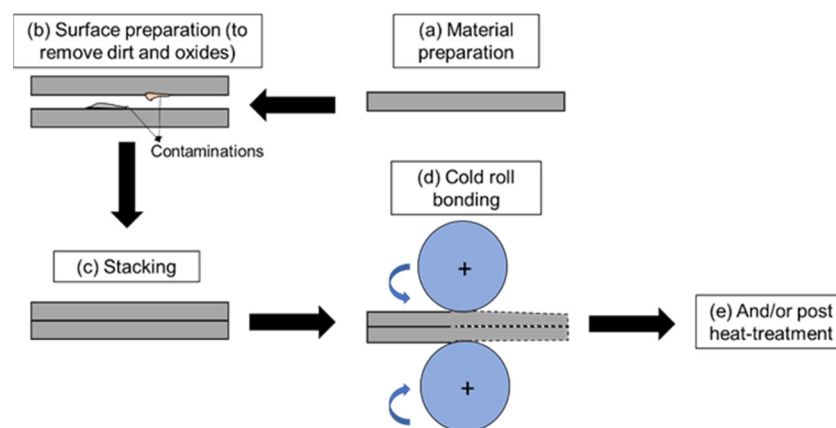

Figure 1. Steps involved in the CRB process.

2.2.2. Hot Roll Bonding (HRB) Process

The HRB process is categorized as when the processing temperature is greater than the recrystallization temperature [21]. The process is also known as the heat and pressure process and has seen advancements since its introduction in the 1980s. The process setup is similar to CRB, except that the sheets are preheated before passing through the rollers, often in a vacuum environment. The process starts with surface preparation of the materials, then preheating the sheets into their plastic range, after which the stacked sheets are passed through rollers where the close contact between stacked materials produces interfacial bonding. It is an established process that can join carbon steel and stainless-steel claddings. The warm roll bonding process is similar to hot roll bonding, except that the processing temperature remains close to the recrystallization temperature.

2.2.3. Accumulative Roll Bonding (ARB) Process

ARB, patented by Saito et al. [22], is a rolling process where a severe plastic deformation (SPD) is applied to obtain ultra-fine grain (UFG) structures during bonding multiple sheets. In the ARB process, pre-rolled sheets are sectioned into halves, surface treated, stacked together, and then subjected to the rolling process numerous times to achieve ultra-fine grains (UFGs). The stacked sheets can be subjected to pre-, post-, and inter-rolling heat treatment cycles to obtain the desired microstructure and properties. Figure 2 illustrates the ARB process, where only the first two steps are shown for illustration (the reduction in thickness is 50%). The process follows the same cycle until the desired deformation is achieved. The ARB process can be performed with and without heating of the worksheets and, therefore, not categorized as a CRB or HRB process. Moreover, it is important to note that the research on the ARB process is mostly focused on grain refinement mechanisms, and limited work has been carried out evaluating the joining phenomenon taking place during the process [23]. However, for the present review, the ARB process is included among the RB processes, as an interfacial metallurgical bond occurs during the process. Table 1 provides a comparison of the RB processes.
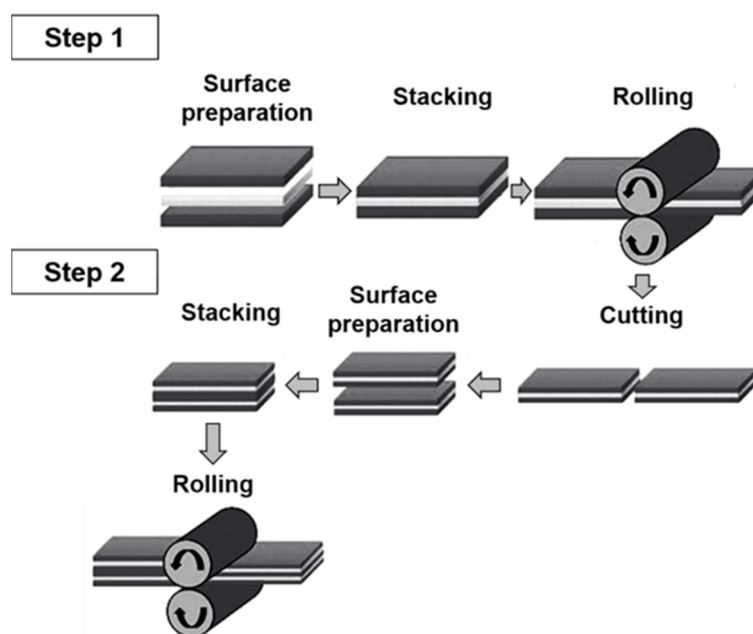
Figure 2. Schematic diagram of the ARB process.

Table 1. Comparison of roll bonding (RB) processes.

RB Process	Operating Conditions	Key Process Variants	Process Features
Cold roll bonding	T_p < Recrystallization temperature	Cold pressure welding by rolling	Severe plastic deformation is achieved without heating generally at high pressures.
		Clad sheet by rolling	
Hot roll bonding	T_p > Recrystallization temperature		- Sheets can be heated pre-, post-, and inter-rolling cyclesto obtain tailored microstructure. - Hot rollers are used during the rolling cycles for obtaining the ductility and tailored microstructure.
Warm roll bonding	T_p = beginning of Recrystallization temperature		Sheets are pre-heated close to half of melting temperature to soften the material.

where T_p = Processing temperature.

Looking at the processes' mechanics in Table 1, the CRB process emerges as being simpler and more inexpensive than the HRB process, as no heating is involved. Furthermore, the lack of heating in CRB inhibits the thermal effects on the bonded sheets. As the process is performed at room or low temperature, no undesirable microstructural changes and phase formations (such as brittle intermetallics in the case of dissimilar materials) are expected. However, the CRB process requires careful surface preparation, as the main bonding mechanism is adhesion, which is difficult to achieve without a controlled environment. Consequently, high pressure over a long time is required to achieve a good quality joint. Furthermore, the requirements of surface preparation and the close placement of joining sheets restrict the thickness of the joining sheets. These stringent requirements are not necessary for the HRB process. It can be inferred that for the joining of thick sheets and where the controlled environment is difficult, the HRB process can be preferred while for the thin foils, multi-layer thin composite structures, and where high plastic deformation is a prerequisite, the CRB process can be implemented. In the proceeding section, bond formation mechanisms for both processes are presented to better understand the application of each variant.

2.3. Bond Formation Mechanisms

Based on the type of variants, four popular theories are widely accepted to explain the bonding mechanism in RB processes. These include film theory, energy barrier theory, diffusion bonding theory, and joint recrystallization theory.

The film theory is based on the disintegration of surface layers during the rolling process. Disintegration exposes the underlying material, which is further extruded through the cracks of the oxide layer or work-hardened surface layer under the application of rolling pressure. Researchers [24] have suggested that film theory is most relevant for explaining CRB as the process operates at low temperatures and primary bonding is formed because of attraction forces between atoms rather than diffusion bonding. However, an energy barrier needs to be surmounted to bring two constituent material surfaces into contact. This requirement leads to the energy barrier theory, which states that there is a minimum energy essential for rearranging the surface atoms, and the dispersion of surface oxide particles. The other two approaches, diffusion bonding, and recrystallization theory are more related to HRB as recrystallization and interatomic diffusion are considered to explain bond formation at elevated temperatures.

2.4. Research Needs

Bonding mechanisms are well understood and have been extensively researched for traditional joints. However, for multi-layered joints, the layer-wise bonding mechanism, the bond variation throughout the joint, and the extent of bonding between the subsequent layers during RB are not well understood. Predictive models and experimental programs are required which can estimate the extent of joining throughout the joint and the bonding mechanism between different layers and different material combination with change in the processing parameters.

3. Characterization and Evaluation

3.1. Key Process Parameters

Extensive research has been conducted over the years to ascertain the critical parameters involved in RB processes. Although the critical parameters differ slightly from one RB variant to another, the research community agrees that some of the key parameters such as thickness reduction, rolling speed, surface preparation, and heat treatment/annealing conditions are common which affect the joint quality and strength. Figure 3 provides an overview of the variables in RB processes and how they are shared among different variants. A detailed discussion of the key process parameters is presented in the next paragraphs.
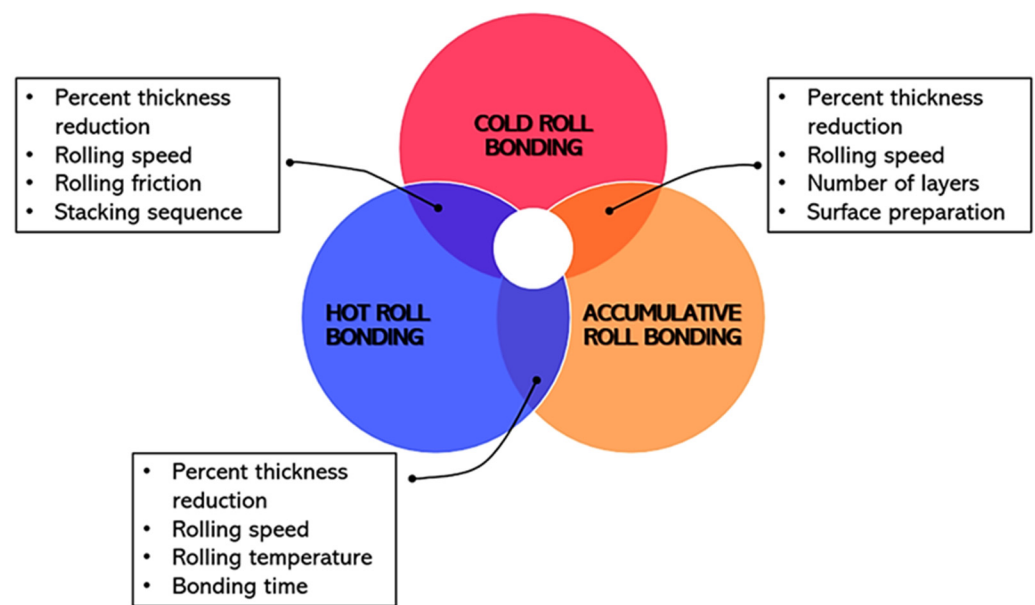
Figure 3. An overview of the similarity variables with regard to process parameters in RB processes.

3.1.1. Percent Reduction Factor

The majority of authors [25–27] have agreed that percent reduction factor, i.e., the change in thickness after the application of the RB process, is considered to be the most crucial parameter. Initial studies [28] have suggested a strong relationship between bond strength and percent reduction value. Improved bond strength has been observed in experiments with an increase in the threshold reduction [25,29], translating into an increase in the area fraction of cracks, and an expansion of surface due to the increase in rolling pressure. However, a deformation threshold defined as "R_t" exists for every metal in order to obtain a good bond [30,31]. After reaching the "R_t" limit, a rapid decrease in bond strength occurs, which gradually stabilizes according to the strength of the weaker material involved in the joint formation.

3.1.2. Rolling Speed

Rolling speed is arguably one of the most critical process parameters, and alone and/or in combination it can affect the joint interface, microstructure, and mechanical properties. The results of studies investigating the effect of rolling speed [31,32] revealed that rolling speed has a direct relationship with "R_t" value. This phenomenon has been attributed to the inadequate extrusion of the parent materials through oxide layer cracks due to the short processing time. In reality, rolling speed has a two-fold effect on the process. High rolling speeds can lead to high temperatures useful for good joint quality, but at the same time, it results in a compromise on duration needed to allow sufficient bonding [33].

3.1.3. Surface Preparation

In practice, most material surfaces have different oxide films and adsorbed contaminants that prevent strong bonding. Therefore, surface preparation conditions are important considerations. Several authors [34,35] have investigated the surface preparation conditions to achieve good quality roll bonding joints. It was found that "R_t" values dropped as the thickness of oxide film was reduced [36]. Surface preparation for roll bonding joints can be categorized into three classes: (a) mechanical cleaning; (b) formation of a brittle cover layer; and (c) chemical cleaning [37]. Through experiments, it has been observed that scratch brushing in combination with degreasing yields optimal bonding strength. However, the reverse sequence resulted in higher "R_t", and consequently, lowered bonding strength [35]. Surface roughening by scratch brushing [38] significantly enhances the

joint quality by reducing the pressure necessary for initiating bond formation. It has also been found that shear displacement is necessary for bonding even when two oxide-free surfaces come in contact with each other [39]. This hypothesis was put to the test in another investigation [40], where the researchers selected gold (as it has no oxide film) to form roll-bonded joints. It was found that gold samples did not establish a bond under the pressure, whereas bonding was established in wire-brushed specimens. The authors cited the absence of local deformation as a cause for the poor quality of bonding. In another study, Agers et al. [41] found that the local interfacial deformation appeared to be more crucial than the macroscopic deformation.

3.1.4. Heat Treatment

The heat treatment of roll bonded samples also emerged as an essential step and can further be classified into pre-, inter-, and post-processes. Less research has been conducted on pre-heat procedures than on post-heat treatment. Researchers have observed improved strength after performing pre-rolling annealing for joining of Al-1100 alloy sheets, and the effect was more evident at higher reduction thresholds. The authors determined that pre-rolling annealing enables the disintegration of the surface oxides and increases the formability of underlying parent metals. Consequently, more extrusion occurs through the cracks of oxide layers thereby improving the bond strength [42]. Pre-rolling annealing also provides the necessary energy required to start the bonding process [25]. The effects of post-heat treatment for CRB samples of aluminum, copper, and steel [43,44] indicated that short-time heating at low temperatures before the start of recovery and recrystallization increases the bond strength owing to (a) decreased hardness and greater bond toughness, (b) enhanced thermally activated short-range atomic movements at the interface and atomic diffusion phenomenon, and (c) reduction in the residual stresses between the solid-state bonded materials.

In summary, it can be deduced that threshold reduction, surface preparation, and heat treatment processes are the most relevant process parameters. Joint strength increases as reduction increases due to the decrease in the threshold deformation value. Both pre-and post-rolling annealing treatments improve the bond strength owing to the disintegration of the oxide layers. The rolling speed effect depends on the combined influence of temperature and contact time. In addition to the above discussion, other important aspects/parameters, like the type of constituent material (single or multi-phase) [20], the bonding temperature in hot roll bonding [45–47], the bonding time [48], the stacking sequence [49], the geometry of the deformation zone [50], the number of layers and their thicknesses [51], and the lattice structure [17] were also investigated under the rolling condition parameters. Figure 4 presents the critical process parameters involved at each step of the RB process.

3.2. Research Needs

With respect to process characterization, the literature suggests that most of the key process parameters have been established. However, for any joining process, process monitoring and control, and key quality attributes of the joints are governing elements that determine the technological readiness level of the process [52]. For this purpose, a detailed definition of quality attributes concerning process parameters is lacking for RB processes. In addition, however, despite the advances in hot RB processing, defects and inconsistent joint quality, especially in ultra-thick plates (among other challenges), hinder its easy adoption by key industries. In this material processing context, machine learning can be leveraged to develop and optimize process parameters instead of the conventional design of experiments approach which tends to be expensive and time-consuming. In a similar vein, no standards or guidelines are available for in situ process monitoring and control. Such guidelines are required to identify systematic or random events because of process variations, arbitrariness, or process degradation. A feedback control mechanism can be further formulated to mitigate such deviations.
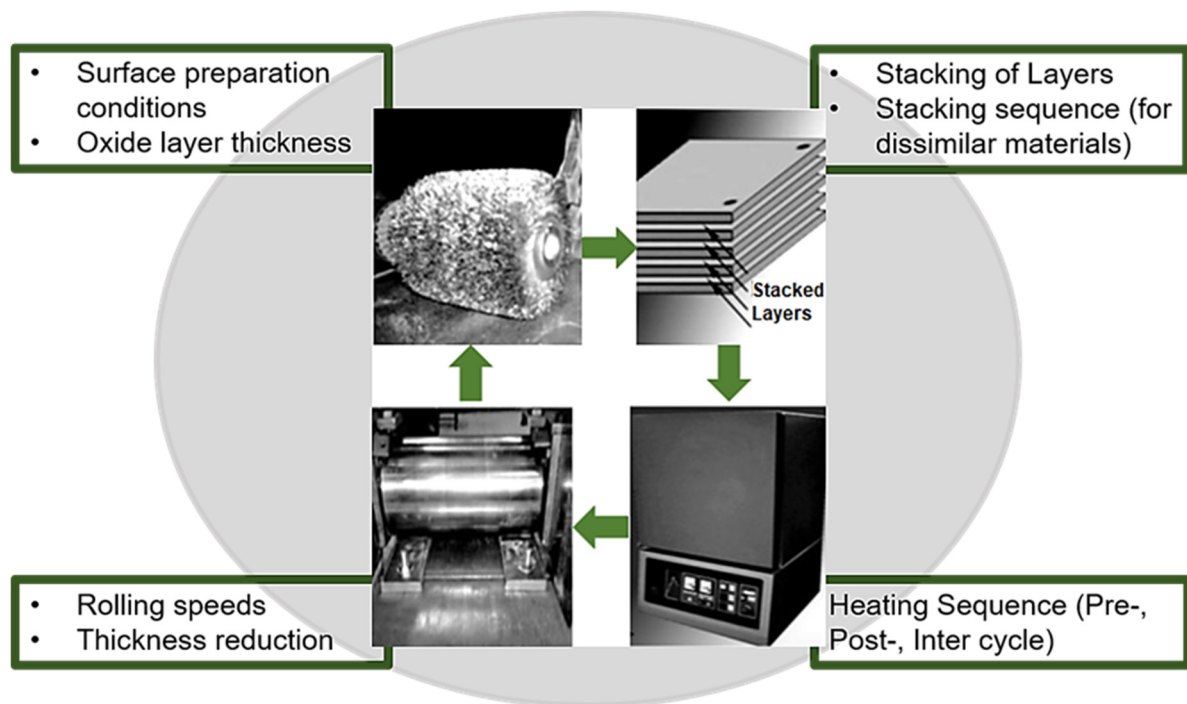
**Figure 4.** Critical process parameters in different steps of the RB process.

3.3. Joint Evaluation

3.3.1. Microstructural Characterization

Microstructural evolution occurs in different ways for various RB processes depending on the material configuration, process parameters, and process dynamics itself. In the case of CRB and HRB of similar materials, diffusion and plastic deformation occurs at the interface which defines the joint quality and the microstructure of the individual sheets. In the case of HRB of dissimilar materials, the interfacial microstructure is of paramount significance, as it defines the bonding between the sheets. In ARB of similar materials, SPD-driven recrystallization leads to an ultrafine grained microstructure, achieving the desired tailored properties.

For ARB processes, UFGs (100 nm to 1 μm) are the most sought-after grain structure. However, the grain refinement can occur due to either plastic deformation and/or recrystallization. For instance, during an ARB process of Al2/Al5N laminates, recrystallization (sharp color grain in Figure 5a) is observed until eight ARB cycles, along with UFG due to plastic deformation which are shown through gradually changing colors in Figure 5a [53]. However, the authors observed the absence of recrystallized grains after 10 ARB cycles (Figure 5b). The authors reasoned that with an increasing number of ARB cycles, the retarding force increases to the extent that it stops the grain boundary movement, thereby inhibiting recrystallization. On the other hand, in the case of HRB of multiple materials, in addition to the evolution of the joint microstructure, the aspects of diffusion of species must also be understood. For example, Liu et al. showed that in stainless-steel clad plates, diffusion distances of Fe, Cr and Ni gradually increase, and as a result the interfacial shear strength also increases when rolling is carried out at higher temperatures; for example, in this case the rolling temperature ranged from 1100 to 1300 °C, as shown in Figure 5c–e, taken from Ref. [54]. In addition, the SEM micrographs shown in Figure 5f–h, taken from Ref. [55], represent the bonding interface of a hot-roll-bonded titanium alloy/low-carbon steel plate, with significant grain refinement evident as the reduction ratio is increase. These microstructure modifications and the compound layer formed at the interface at high heating temperatures and higher reduction ratios can often be the controlling factor that determines the resulting strength of a joint.
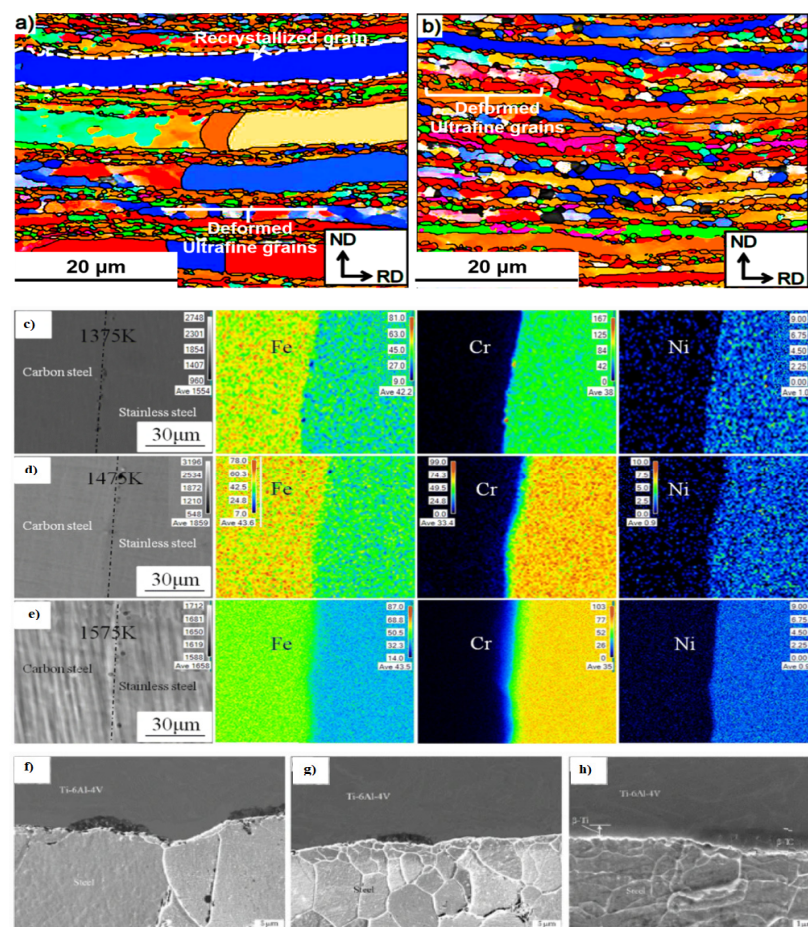
Figure 5. Microstructure evolution in Al2N/Al5N composite joint (**a**) after 8 ARB cycles (where white dashed line is showing one of the recrystallized grains with the presence of deformed UFGs), and (**b**) after 10 ARB cycles, where recrystallization is absent, adapted from Ref. [53]. (**c–e**) HRB macrostructure and elemental maps showing the interfacial alloying elements maps of stainless-steel clad plates rolled at different temperatures adapted from Ref. [54]. (**f–h**) Microstructure of dissimilar hot-roll-bonded interface at 1050 °C at 36, 58, 70% reduction ratio, adapted from Ref. [55].

Wu et al. [56], while investigating Mg/Al laminated ARB joints, noted that during processing, Mg layers retained their coherency while the Al layer underwent necking and subsequent fracture. Two phases of the intermetallic compound (IMCs) were observed, Mg_2Al_3 near the Al layer and $Mg_{17}Al_{12}$ in the vicinity of the Mg layer. A similar phenomenon was reported by Hebert and Perepezko [57], where the authors concluded that there was a rapid growth of intermetallic throughout the ARB process, which could be fractured easily. Huang et al. [58] investigated the ARB of pure aluminum joints and found the growth of a sub-micrometer lamellar structure at high strains. The sub-micrometer structure was found homogeneous throughout the coupon thickness. Similar findings have been reported in previous works [59,60].

In HRB of similar stainless-steel clad joints [54], the interfacial bonding was solely attributed to the diffusion behavior of Fe, Ni, and Cr elements, and stronger shear strength was observed for larger thickness of the diffusion layer. In another study [20], AZ31/CP-Ti clad joints were manufactured by heating Ti sheets only through same temperature rolling (STR) and differential temperature rolling (DTR), resulting in a straight bonding interface and a corrugated bonding interface with a serrated-shaped morphology for STR and DTR joints, respectively. Yi et al. [61] reported the formation of fully recrystallized and large-grown grains due to an intermediate annealing step during hot rolling. Furthermore,

Zhang and Acoff [62] demonstrated that high rolling strain prompts accelerated diffusion in the multilayered composite layers, thereby resulting in more intermetallic compounds.

Li and his co-authors [63] examined the microstructure development of ultrafine-grained Al/Cu laminated composites produced through asymmetric CRB. They observed a tight bonding interface because of significant plastic deformation as shown in Figure 6a. High-temperature annealing accelerated the atomic diffusion but also resulted in the intermetallic compounds formed at the interfacial layer as shown in Figure 6b. The solid solution strengthening effect was also observed at 300 °C. It can be inferred that the resultant microstructure in CRB and HRB processes is dependent on the previously discussed process parameters and the resultant state functions (temperature, sheet threshold reduction, strain, etc.) and eventually material configuration (i.e., similar, or dissimilar materials).
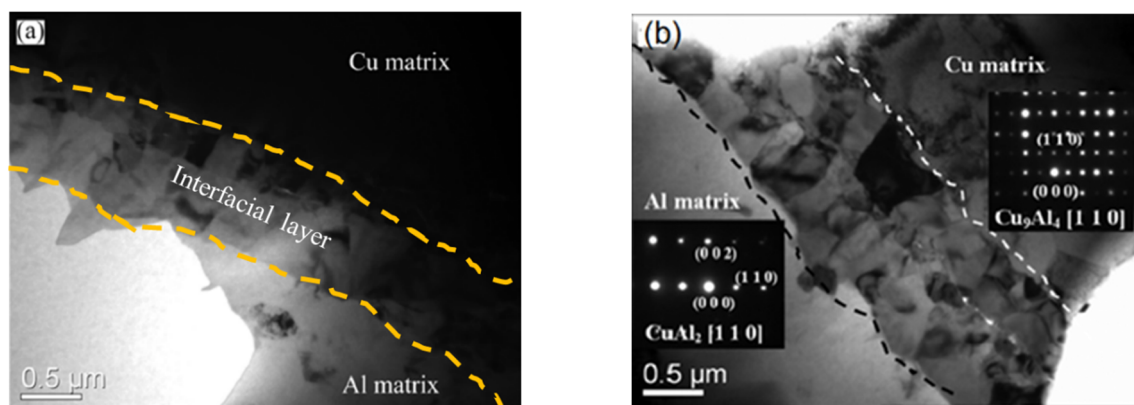
Figure 6. (**a**) Tight formation of bonding interface after cold rolling, and (**b**) atomic diffusion and intermetallic formation at the interface after annealing at 300 °C. Reproduced with permission from Ref. [63].

Figure 7 summarizes the overall microstructural evolution mechanism in RB processes. Although recrystallization is a common phenomenon in both configurations of the material, the recrystallization mechanism can be different for the two cases. Static recrystallization has been found to be more dominant in similar metal joints processed through CRB than dynamic recrystallization in dissimilar metals RB joints processed through HRB/ARB. Moreover, the morphology and extent of the diffusion layer and the nature/formation of intermetallic compounds (IMCs) are linked to the rolling temperatures, number of rolling cycles, and heat treatment (HT) conditions.

3.3.2. Research Needs

Microstructural evolution phenomena have been well studied for RB processes. The problem arises in the case of dissimilar materials, where thick IMC layers lead to joint degradation. Consequently, controlling the heat input during the process is critical. Placing an interlayer between the two sheets has shown promising results in this regard [64], and could be extensively further explored. In addition, maintaining constant pressure throughout the process is important to achieve a uniform microstructure. For this purpose, in situ microstructural studies involving closed-loop temperature and pressure measurements are required to observe the new phases and microstructure formation. Such studies can be further used to optimize the process parameters in a manner so the growth kinetics of IMCs can be slowed.

3.3.3. Mechanical Evaluation

Mechanical behavior helps in accessing the performance of a joint structure during its service life. This section gives insight into the joining capability of different metals through RB processes.
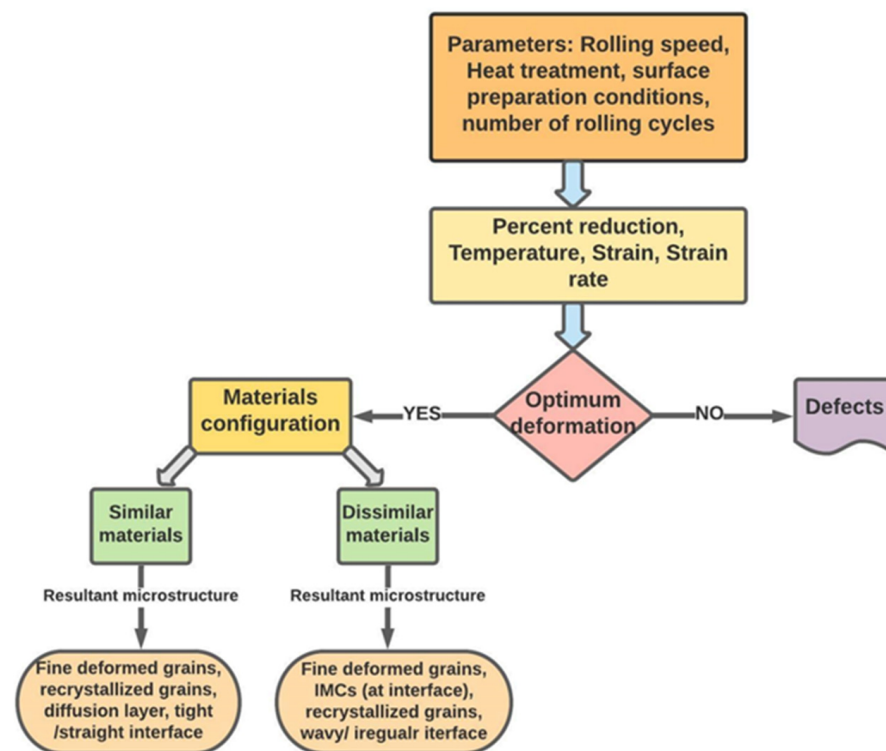
Figure 7. Overall microstructural evolution in RB processes.

Chekhonin et al. [65] found that for ARB processed aluminum laminates, yield strength, and ultimate tensile strength increases with increasing number of processing cycles. The authors reasoned that this rise in strength was related to grain refinement and intensification in the dislocation density. Researchers [56] investigated the tensile strength of Mg-Al ARB laminated composites which were preheated in both rolling and transverse directions before the process. During the ARB processing of pre-heated samples, tensile strength and elongation decreased significantly in the rolling direction despite initial increase along with strong anisotropy in yield strength. The authors reasoned that necking and rupture happened in the hard layer with subsequent ARB cycles, as instabilities originating from the variances in the parent metals caused fracture of the Al layer, and the remaining strength provided by Mg layers was insufficient to prevent deformation around the Al layer, resulting in degradation in strength. Researchers [66] investigated the joint efficiency of hot vacuum roll bonded Zr–AISI 321 and Zr–C22E steel joint and found greater joint strength than in the less durable material in both configurations. Luo et al. [67] joined Ti to stainless steel with Nb as an interlayer using HRB. The authors observed degradation in tensile strength with increasing temperature because of enhancement in the volume fraction of the IMCs. A similar trend was noticed by Saboktakin et al. [68] when investigating the mechanical properties of HRB Fe-Ti joints with copper foil as the interlayer.

Microhardness tests have been conducted by many researchers to investigate the interface-local mechanical properties. Figure 8a [11] shows the plot for hardness vs. "R_t" values for similar metals while Figure 8b [11] depicts the plot between hardness ratio (hardness variation between two constituent metals) and "R_t" values for CRB joints of dissimilar metals. Figure 8a shows an increasing trend as hardness value increases in similar materials joint. It can be inferred from the analysis that a higher value of "R_t" is required for the bonding of harder materials. From Figure 8b, it can be inferred that the "R_t" value decreases with the decrease in hardness ratio, thereby improving the bonding mechanism.
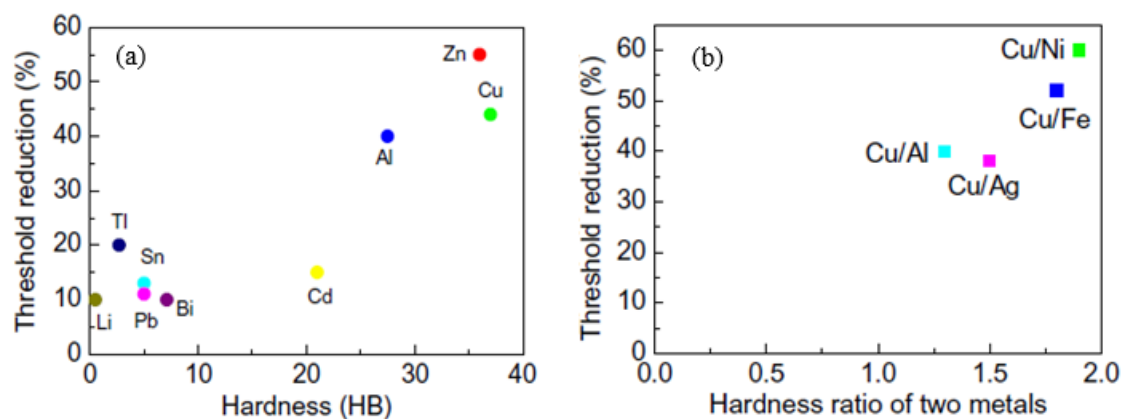
Figure 8. (**a**) Hardness and "R_t" relationship for same metal CRB joints; and (**b**) hardness ratio and "R_t" relationship in dissimilar metals CRB joints. Reproduced with permission from Ref. [11].

In summary, it is noticed that the tensile and the yield strength show a contrasting pattern in the variants of the RB process. For the HRB, the tensile strength decreases with increasing temperature and the number of rolling cycles as a result of the formation of interfacial intermetallics and their subsequent fracture due to the applied load along with grain growth. However, for the CRB, the tensile strength improves with an increment in the number of cycles, as a consequence of grain refinement and increased plastic deformation.

3.3.4. Research Needs

Different testing methods such as tensile, shear, multistep shear, and peeling tests are available for the quantitative evaluation of RB joints whereas several tests (impact, fatigue) for the qualitative evaluation for thick sheet joints are present as well. However, mechanical evaluation of thin sheet joints poses a challenge due to the involvement of different metal combinations. Moreover, for dissimilar metals joints, interfacial properties are critical, but no existing standard provides a guideline for their measurement. The development of such guidelines while taking aid from non-destructive measurements can be beneficial for improving the mechanical performance evaluation.

3.3.5. Defects in RB Joints

Defects in RB joints can occur due to various reasons such as the selection of inappropriate processing parameters (rolling speed, number of passes), material configuration (i.e., similar, or dissimilar materials), environmental effects (oxide layer formation), and heat treatment temperatures. However, due to the distinct process mechanics of the two main variants of the RB process, i.e., CRB and HRB, some of the defects are peculiar to a specific process, such as brittle intermetallic fracture in the case of HRB. Furthermore, it is important to note that in RB joints, almost 81% of the defects can be categorized as bond/interfacial defects [69]. Therefore, the focus of this review will be on defects related to bond strength.

Interfacial gaps/voids between the two joining sheets are the most common defect observed in both CRB and HRB processes. For the CRB process, the interfacial gap is linked to the absence of the metallurgical bonding due to a lack of requisite plastic deformation as explained in [70]. The authors found that the sheet thickness and threshold reduction "R_t" are the main causes of this defect. It is explained that the SPD may occur during the rolling process of Al-Fe which can lower the vacancy activation and migration energies, thereby significantly promoting the diffusion phenomenon. The diffusion yields in the formation of an interfacial diffusive layer thereby form a metallurgical bond. However, the prerequisites for the formation of such a diffusion layer are the achievement of a threshold "R_t" value and the joining of thin sheets. The presence of a fractured/brittle oxide layer (environmental effect) also hinders the formation of a strong interfacial bond in roll-bonded

joints. This can be explained by the interfacial brittle oxide layer fracturing when subjected to stress during the rolling process. Moreover, the variation in mechanical properties between the workpiece materials and oxide layer results in instabilities during plastic deformation. Consequently, necking and fracture in the oxide layer occur and the interface consists of weak oxide fragments [71]. It has been established that the bond strength is inversely proportional to oxide layer thickness.

Brittle intermetallic formation at the interface mostly related to rolling bonded dissimilar materials joints can also be regarded as a defect, as it degrades the joint bonding strength. The intermetallic layer thickness, if not controlled, can severely affect the joint strength as observed in [72]. The thickness of the intermetallic layer can be controlled by carefully selecting the pre-, post-, and inter-rolling heating cycles/temperature. Porosities and cracks in the interfacial layer are also observed in the HRB joints where different IMCs are formed at the interface as a result of the dissociation of one IMC to others at prolonged annealing times/cycles [73]. Furthermore, porosities are pronounced due to the presence of simultaneous other mechanisms, such as the formation of Kirkendall voids because of the vacancies diffusion toward the interface, and the dissimilar contraction behavior of the IMCs during the cooling period results in voids and cracks between some layers. It can be inferred that the defects in the RB joints are more inherited from the process-control than the process dynamics. The defects in the preceding paragraphs are critical to joint performance in terms of peel resistance, fatigue resistance, and enhanced tensile strength. Table 2 provides a summary of the defects with their related cause in terms of process parameters. Careful selection of process parameters and their subsequent optimization is therefore critical for obtaining a sound joint.

Table 2. Common defects in RB processes.
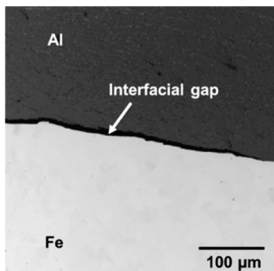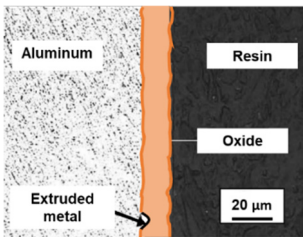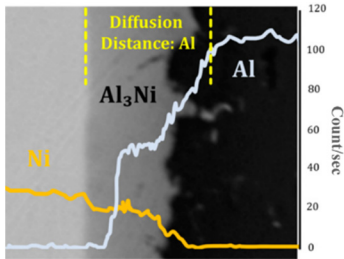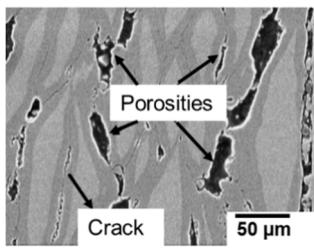
Nature of Defect	Key Process Parameters	Defect Morphology	Reported by
Interfacial gaps	Rolling speed Sheet thickness		Wang et al. [69]
Presence of oxide layer	Surface treatment		* Le et al. [70]
Brittle Intermetallics	High rolling temperatures and/or high post or inter-rolling cycles HT temperatures		** Azimi et al. [71]

Table 2. *Cont.*

| Nature of Defect	Key Process Parameters	Defect Morphology	Reported by
Porosity and cracks	Prolonged heat treatment cycles	Porosities / Crack 50 µm	Mozafferi et al. [72]

* The color of the oxide layer is altered for ease of understanding. ** The curves on the monograph represent a line scan for an indication of chemical composition, where the IMC phase exhibits constant chemical composition.

3.3.6. Failure Modes Relationship with Ductility and Formability

Roll bonded sheets, especially cold roll bonded sheets, of dissimilar metals, normally exhibit loss of ductility and require annealing at higher temperatures to improve their formability. However, annealing at higher temperatures may result in the formation of brittle IMCs at the interface. These intermetallics can act as internal inclusions and defect sites to initiate failure. Hong and Weil [74] conducted tensile and bend tests on niobium-clad stainless-steel sheets. Through chemical analyses, they observed the presence of iron-niobium (FeNb) intermetallic compound at the interface due to annealing treatment which caused the failure in bend test and tensile test specimens. In a follow-up study by one of the authors of this paper, the effects of annealing conditions on the ductility and formability of niobium clad stainless-steel sheets were investigated [75]. In that study, microstructural analyses and nanoindentation tests indicated formation of brittle intermetallic layer in specimens that were annealed at elevated temperatures. This intermetallic layer caused a failure during bend and flattening tests through localized necking.

Roll-bonded sheets develop anisotropic mechanical behavior, causing a mismatch of strains in different layers under loading. This phenomenon is more pronounced for larger strains corresponding to the plastic range such as those encountered during the manufacturing processes of drawing, forming, bending, and extrusion. Choi et al. [76] investigated the warping of specimens during the tensile deformation of stainless-steel-clad aluminum bilayer sheets. The authors used an iso-strain analytical method along with a finite element model based on anisotropic failure criteria to explain the warping phenomenon. Warping of specimens was also observed during tensile tests in the investigation conducted in [75]. Examples from that work are shown in Figures 9 and 10. The curvature of the cross-section of the failed tensile test specimen in Figure 9b is due to the warping of the specimen under longitudinal loading. It is to be noted that the niobium layer is towards the outside of curvature.

(**a**) Stainless steel layer / Niobium lay

(**b**) Stainless-steel layer / Niobium layer / 100 µm
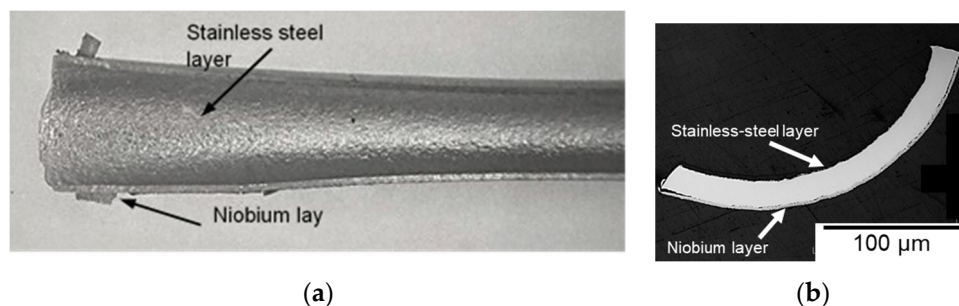
Figure 9. Warping under tensile loading of niobium clad stainless-steel specimen as indicated by (**a**) the canoe-like profile in the optical image of the specimen, and (**b**) the convex curvature in the optical micrograph of the cross-section along the specimen width.

(**a**)   (**b**)
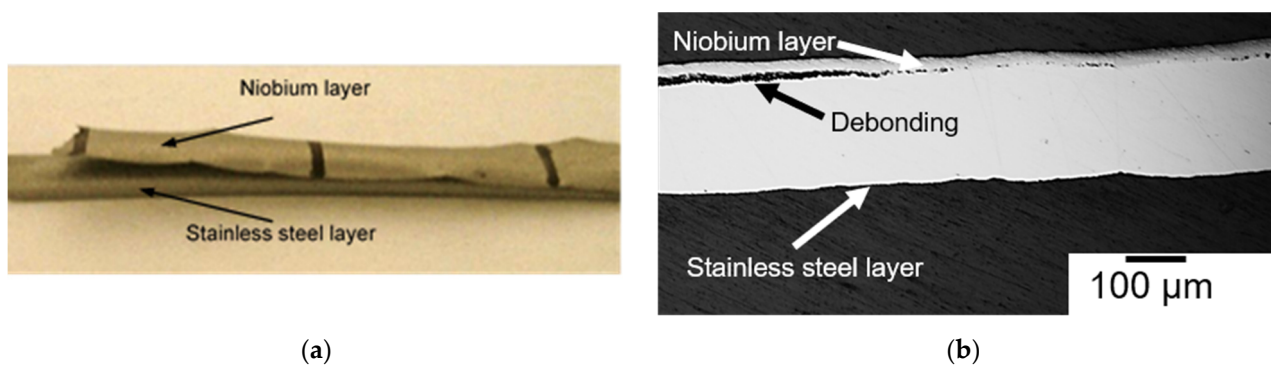
Figure 10. Debonding under tensile loading of niobium clad stainless-steel specimen as shown in (**a**) the optical image of the specimen, and (**b**) the optical micrograph of the cross-section along the specimen length.

Roll-bonded layers of dissimilar metals can also experience debonding or delamination under applied loading due to failure of the interface and loss of adhesion. Matsumoto et al. [77] observed this type of failure in aluminum-clad Mg-Li plates due to the formation of reaction phases at the joint interface. Delamination of niobium layer in niobium-clad stainless steel tensile specimens was also reported in [75] and an example is shown in Figure 10a. The micrograph in Figure 10b indicates a fracture of the intermetallic layer leading to debonding in a tensile test specimen.

3.3.7. Research Needs

The formation of IMCs and the phenomenon of warping and debonding have been reported for roll-bonded metal sheets of dissimilar materials. This may necessitate the establishment of new guidelines and criteria to determine the ductility and formability of roll bonded dissimilar metals. It would be an interesting research topic to formulate forming limits incorporating anisotropy of mechanical properties arising from the roll bonding of dissimilar metals. The failure modes in roll bonded metals are also different than those in an isotropic or homogeneous material. Investigation of these failure modes and development of new failure criteria also seems to be an area open for future research.

3.3.8. Electrical Evaluation

Various studies have been conducted to examine the electrical properties of roll-bonded materials. Kang et al. [78] examined the post-heat treatment effect on the electrical conductivity of hot-roll bonded α-brass-clad Cu–Cr composite joints. The results showed better electrical conductivity values at higher post-heat treatment (HT) temperatures. The researchers suggested that those higher temperatures aided by increasing precipitation in Cu–Cr, as well as weakening the dislocation accumulation as the solute atoms (electron-scattering sites) left the solid solution with an increase in temperature. This precipitation phenomenon decreases the total number of electron scattering sites, thereby increasing the electrical conductivity. Abbasi and coworkers [59] examined the influence of the interfacial intermetallic layer on the electrical conductivity of cold roll bonded Al/Cu joints. The thickness of the intermetallic layer was varied by changing the annealing time (post-process HT). The electrical conductivity of the joints decreased with increasing intermetallic width. Yao et al. [79] investigated the electrical conductivity of Cu/C ARB samples and found that the refinement, layer reduction, and distribution of graphite particles improved the electrical conductivity to about 90% of base pure Cu. Figure 11 presents electrical conductivity versus hardness plot for different dissimilar Cu-based roll bonded joints.
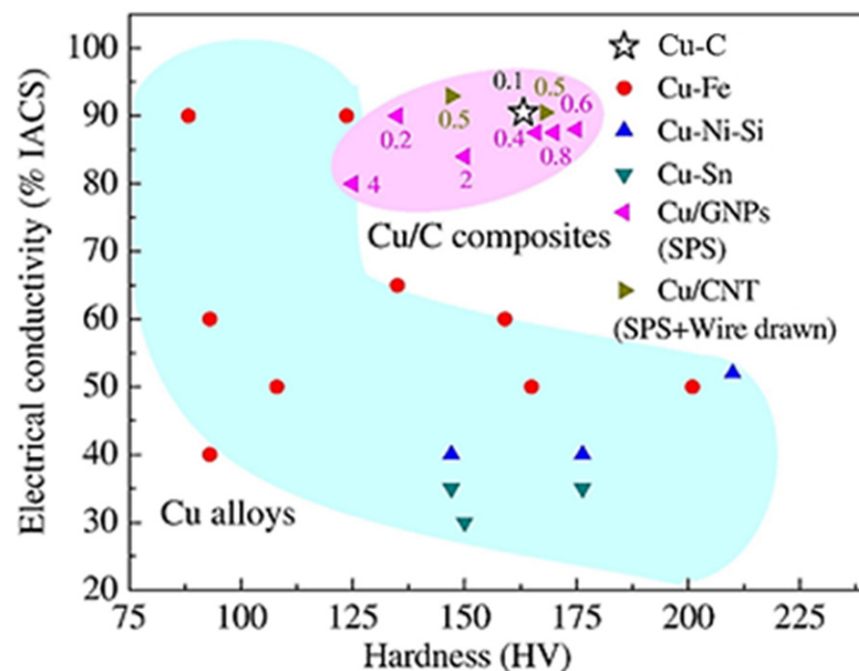
Figure 11. Electrical conductivity vs. hardness plot for dissimilar Cu-based roll bonded joints. Reproduced with permission from Ref. [79].

The electrical properties of the roll-bonded joints are found to be influenced by many factors including the formation of the intermetallic layer which in turn is highly dependent on the process parameters, for instance, rolling speed and temperature. Moreover, electrical properties depend on the type of process itself, for example, layer threshold reduction in the ARB process can significantly improve the electrical conductivity as compared to conventional roll bonding processes.

3.3.9. Corrosion Evaluation

Corrosion resistance is an important consideration, mainly when joining dissimilar materials. Few studies are available in the literature explaining the corrosion-resistant nature of roll-bonded joints. Naeini et al. [80] investigated a decrease in pitting corrosion resistance of Al-5052 alloy sheets processed through the ARB. The authors found the formation of the lesser passive film with increased cold deformations because of an increase in dislocation density and defects. Mahdi et al. [81] deduced that the corrosion-resistant properties of the ARB processed Al/nano-silica nanocomposites sheets could be enhanced by augmenting the number of process cycles and some nanoparticles. Khara et al. [82] used CRB to develop a Cr-coating for improving the corrosion resistance of mild steel. The authors claimed that the corrosion resistance of the mild steel is increased similar to 304 stainless steels. In a recent study [83], a comparison was drawn between CRB and ARB joints of AA5083 alloy. Through employing different corrosion characterization techniques, the authors observed that both CRB and ARB joints showed intergranular corrosion (IGC) resistance in as-deformed conditions. However, the CRB joints became sensitive to IGC after 7 days of sensitization at 100 °C and 150 °C (Figure 12a). Interestingly, ARB joints maintained their insensitivity (Figure 12b). The authors reasoned this behavior is related to different morphology and precipitation of the ß phase which occurred during sensitization. It can be noted that after a critical "R_t" value, the corrosion resistance decreased. This phenomenon can be attributed to increased defects and dislocation densities.
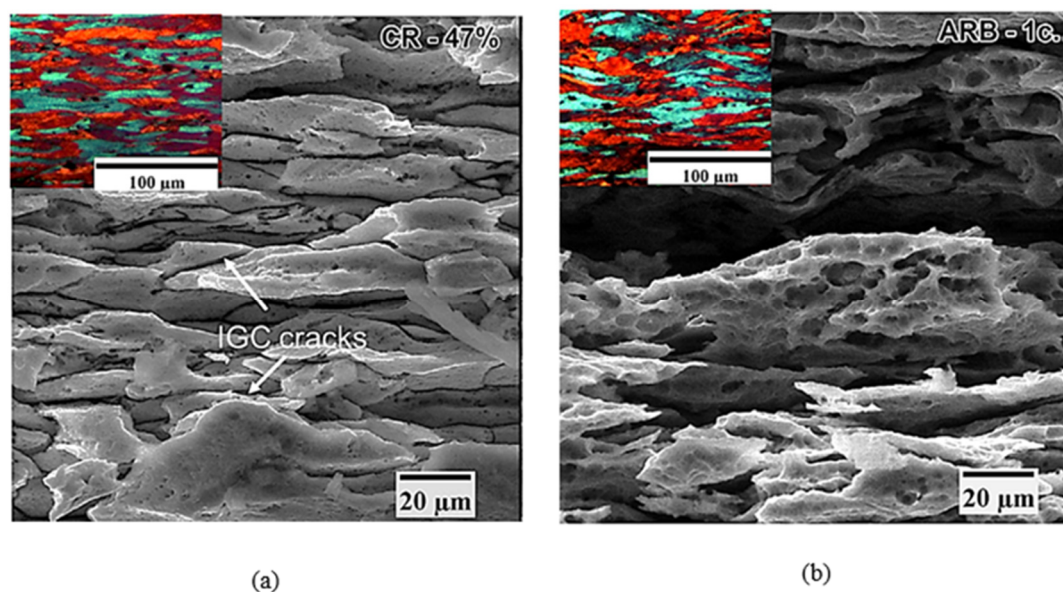
Figure 12. Cross-section surface morphology of (**a**) CR AA5083 alloy, and (**b**) ARB AA50083 alloy after sensitization for 7 days at 150 °C. (The insets in the figures show the grain structure after processing). Adapted from Ref. [83].

3.3.10. Research Needs

Corrosion is still not well understood for dissimilar material RB joints. Although galvanic corrosion is regarded as the most common mechanism in dissimilar materials, nevertheless, the corrosion mechanisms can be more perplexing in RB joints owing to the presence of randomness from processing (e.g., non-uniform pressure), a crevice in the case of lap joints, and the different characteristics of the metals and nonmetals worksheets. Adhesive application may reduce the corrosion effects; however, this application is still in its infancy. Moreover, predictive models that can provide a critical understanding of the structural performance of the RB joints under extreme environments are unavailable. To surmount this research deficiency, reliability and physics-based lifetime models which can effectively envisage the durability and performance of RB joints functional in extreme environments will be beneficial.

4. Modeling and Simulation

Different theoretical models have been suggested to elucidate various aspects of the roll bonding process. Most roll bonding models have focused on controlling the process parameters, while some models have developed the relationship between microstructure evolution and bond strength. The researchers in [24] suggested the following equation for evaluating joint strength.

$$n = \frac{\sigma_B}{\sigma_0} = R_f \left(2 - R_f \right) \tag{1}$$

where "σ_B" denotes the bond strength, "σ_0" is the strength of the base metal, "n" is bond strength efficiency, and "R_f" is the final reduction after rolling pass. In this model, the bonded area is proportional to R_f. Wright et al. [84] presented the theoretical model for bond efficiency regarding threshold deformation and is defined below:

$$n = H(1 - \frac{\left(1 - R_f \right)^2}{\left(1 - R_t \right)^2}) \tag{2}$$

where "H" is the empirical hardening factor, "n" is bond strength efficiency, and "R_t" is the threshold reduction deformation. Hosseini and Kokabi [31] developed a model that can estimate bond efficiency based on the peel test results of Al 5754 alloy. Das and

Nafari [85] used density function formulation to present an analytical model that highlights the significance of electronic interaction in the roll bonding of two metals. Researchers used dislocation density evolution [86] to develop a model that can predict deviation in yield strength and average grain size in ARB passes. Al-AA1100 alloy was processed and tested to validate the results of the model. Researchers [87] analyzed different parameters of the ARB process using a dynamic explicit finite element model. Through modeling, the researchers were able to predict stresses and strains along with the deformation during the rolling process. The model was found to be in good conformity with the empirical results. Several models [88–90] have been constituted to predict the force and torque in joining two to three layers through roll bonding. These models primarily focused on the cladding of metals. In one such study, the slab method of analysis was used to define the deformation mechanism [90]. The model considered two regions in the rolling zone. The first area consisted of unbounded metals where merely the soft metal yielded while in region two, yielding took place in both materials. Other studies [91–93] developed numerical models to predict the process parameters. Researchers developed analytical models [94,95] for the roll bonding of multi-layered bi-metals. The model was based on anisotropy and strain hardening effects in addition to providing information about suitable processing conditions. Recently, researchers have studied the effects of total strip deformation, its initial thickness, the yield stress ratio, and the thickness ratio of the layers on the bonding strength in Steel/Al cold roll bonded joints and found a proportional effect of these parameters on the bond strength [96]. Plastic deformation as a function of rolling time from the computational analysis is presented in Figure 13.
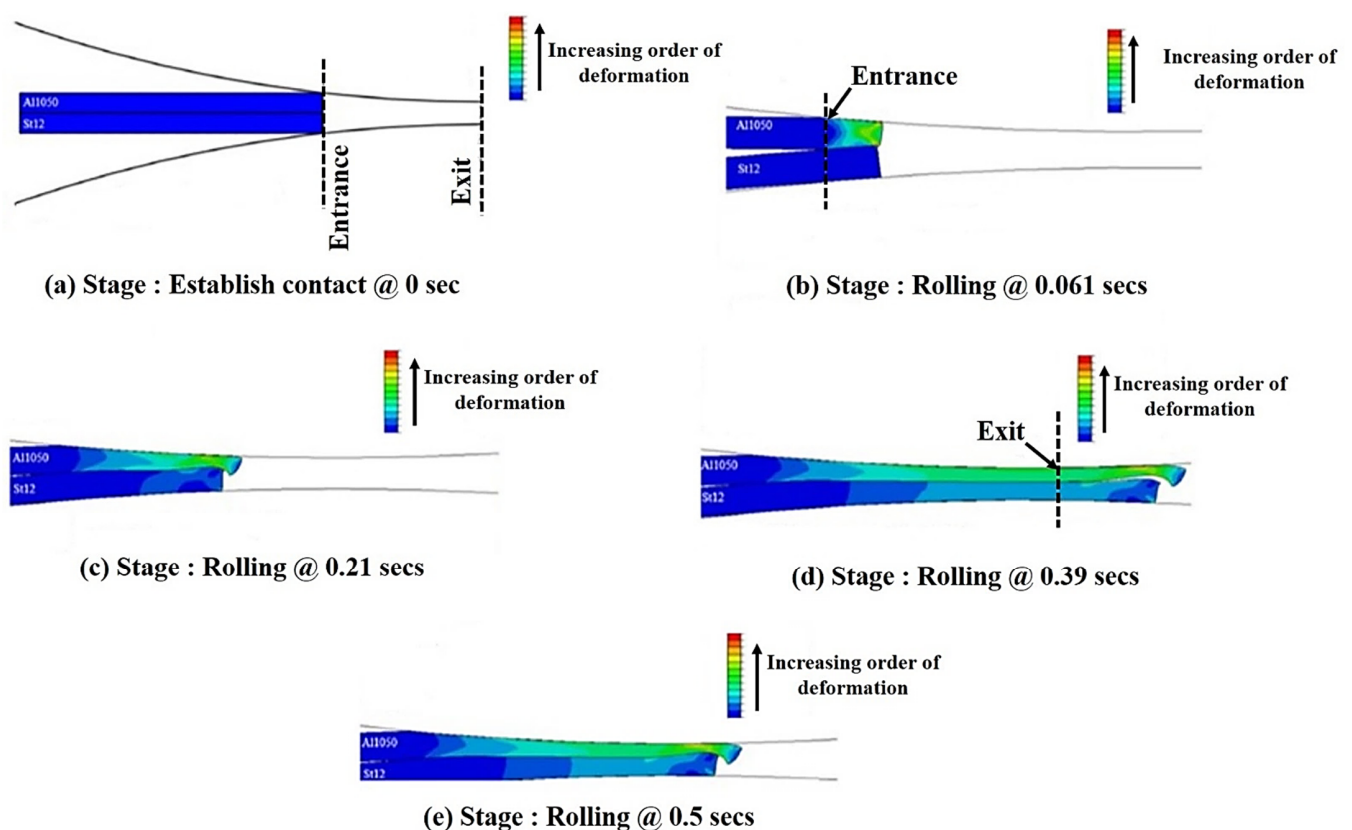
Figure 13. Equivalent plastic strain contours of Fe/Al joints obtained at different rolling times at: (**a**) 0 s, (**b**) 0.061 s, (**c**) 0.21 s, (**d**) 0.39 s, and (**e**) 0.5 s. Reproduced with permission from Ref. [96].

Although several models are available for predicting the roll bonding process, theoretical models have their limitations in predicting the joint strength, especially where dissimilar metals are joined. Numerical models provide better accuracy than theoretical

models but are difficult to use owing to the unavailability of comprehensive data set for different materials and expensive computation efforts.

Research Needs

Material flow and severe plastic deformation are key features of RB processes that render traditional mesh-based numerical simulations ineffective. High-fidelity full-scale numerical models involving fluid dynamics-based Eulerian method or particle-based meshless method may be used to capture the complex metallurgical changes during the joining process.

5. Process Merits and Applications

5.1. Advantages and Limitations

Roll bonding can be used for a wide variety of materials and has been found to work well for joining dissimilar materials [66]. RB process is easy to automate owing to its simplicity and appears as a promising technique for joining foils [97,98]. The ARB process, a variant of roll bonding, can be used to produce ultrafine grains. However, some limitations need to be overcome in order to use the process more efficiently. Surface preparation, which is an important consideration for manufacturing sound joints in roll bonding, is nontrivial to achieve. The limited availability of data regarding the relation of mechanical properties to interfacial bonding has also hindered the use of this process. The bonding mechanism in the hot roll bonding of dissimilar materials requires more extensive research, as the temperature effects during the process have not been fully established. Moreover, the availability of data on the service performance characteristics for roll bonded joints is very limited, making it difficult to compare the roll bonding process with other solid-state processes.

5.2. Applications

Different RB processes have been used extensively for various applications in the past few decades. The ARB process is used for making/joining metallic composite materials in different shapes such as the plate, strip, foil, tube, rod, and wire. These metallic composite materials lend advantages such as low cost and use in multiple applications, including thermal, structural, electrical, and magnetic applications. The joints produced through hot and cold roll bonding are used in different industries. Table 3 indicates some of the different material combinations and their applications.

Table 3. Applications of Roll bonding process.

Material Combination	Applications
Cu/Al	Heat exchangers, electrical components
Cu/Al/steel	Cookware
Ti/stainless steel/Ni	The bipolar electrode in the fuel cell
Nb/Stainless steel	Fuel cell bipolar plate
Cu/Ag	Electrical components and appliances
Al/steel/Al	Automotive exhaust systems

The HRB process has recently found wide application in numerous industries owing to its ability to produce a large area of bimetals through elevated temperature. Particularly, with regard to the joining of dissimilar metals, the HRB process lends advantages such as improved mechanical strength, cost saving, and corrosion and heat resistance [99]. Furthermore, the HRB process exhibits a better adaptability with respect to joining multilayer thick sheets compared to other solid-state processes, such as explosive welding and weld overlay cladding. Carbon steel substrate and stainless steel cladded HRB joints are widely used in different industries, including as pressure vessels, nuclear power equipment, desalination equipment, heat exchangers, armor, bridge engineering, automobile, etc. [100–102]. In a similar vein, Ti, which is one of the most sought-out metals due to its superior strength

and corrosion properties, but for which the difficulty of its processing results in high costs, can be utilized in the form of Ti-Steel composite plates through the HRB process. Ti-Steel multilayer clad plates have gained wide application in the aerospace and construction industries, as well as in nuclear power equipment and heat exchangers [103].

6. Critical Analysis

6.1. Engineering Guidelines

The preceding paragraphs contain instructions regarding the feasibility of material that can be successfully roll bonded. According to the researchers, face-centered cubic (FCC) metals are most appropriate for the cold bonding (CB) process if they are not rapidly work hardened. Al and Cu can be cold bonded most conveniently, while Au, Ag, and Pt can also be cold roll bonded. Hexagonal metals such as Mg, Cd, and Zr have mediocre roll bonding abilities compared cubic metals such as Cu, Al, Pb, and Fe. The bonding properties compared include threshold deformation and maximum strength. Figure 14 presents a metal compatibility map based on different studies on CRB [99–101] and ARB [102–104], which defines the bond formability for various metals through the existing roll bonding processes.
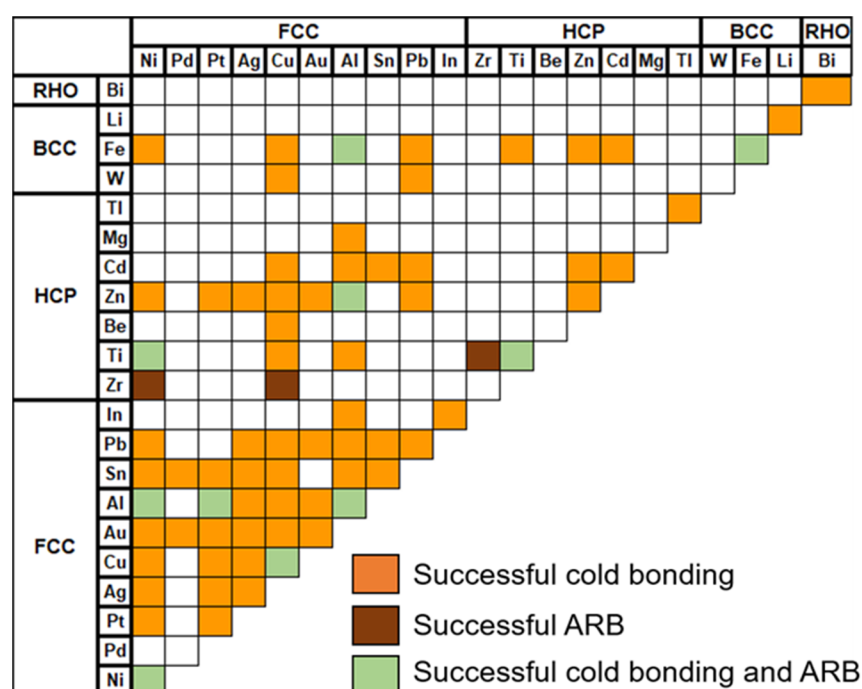
Figure 14. Compatibility mapping for cold roll bonding and ARB. Adapted from Ref. [11].

6.2. Process–Structure–Property (PSP) Relationship

A key aspect of enhancing the technology readiness level of a process is to understand the PSP relationship. This will help engineers and designers in optimizing the process for achieving their desired functionalities. As can be inferred from the previous discussion, RB processes have progressed over the years in terms of both process design and material diversification and have matured to join/develop novel composites in addition to traditional similar and/or dissimilar metals. Table 4 presents a cursory overview of the progress in the ARB process for the last two decades, showing constituent workpiece materials, process parameters, and resultant microstructure and tensile strength.

Table 4. Review of ARB process.

Materials *	Temperature (°C)	No of Cycles	Single Pass Reduction (%)	Grain Information	Tensile Strength (MPa)	Reference
Cu/Ag (nano-cross layered composite)	ˆRT	15	~50	(layer thickness) 20 nm	938 (420% increase)	(You et al., 2021) [105]
Cu	ˆRT	6	60	Dia 1000–2000 nm (sub grain dia 148 nm)	467 (127% increase)	(Eivani et al., 2020) [106]
Cast and rolled sheet of AA2024-[0.5 vol% SiO_{2} p + 1 vol% TiO_{2p}] composite	ˆRT	5	50	70 nm	552 (112% increase)	(Shayan et al., 2020) [107]
Mg-14Li-3Al-2Gd	200	6	50	14.5 μm	229 (78% increase)	(Zheng et al., 2020) [108]
# Al/Cu/Zn/Ni foil (multi-layered composite)	ˆRT	5	50	UFG (no size information)	314 (pure Al had a value 74 MPa)	(Jafarian et al., 2020) [109]
Co (cross layered)	500	5	50	1010 nm	No info about strength [Coercivity 50.2 Oe (60% reduction)]	(Zhu et al., 2020) [110]
Nb-1wt% Zr	700	5	50	800 nm	680 (191% increase)	(Rodríguez-Espinoza et al., 2020) [111]
AA1050/AA5052	RT	7	67	UFG, Dia 350 nm	285 (100% increase)	(Lee et al., 2015) [112]
Al-6061/Ti-6Al-4V	500	1	38	Dia 1200 nm	200	(Ma et al., 2015) [113]
Al/Cu	RT	1	72	UFG, Al 200 nm, Cu 100 nm	290	(Li et al., 2015) [61]
Al/AZ31	280	3	54	Al 1000 nm, 500 nm	475 (Ultimate Bend Strength)	(Liu et al., 2011) [114]
Al/$Al_{2}O_{3p}$ (0.1 vol%)	125	10	50	400 nm	160	(Schmidt et al., 2011) [115]
Al/SiC_{p} (1 vol%)	RT	8	50	UFG, Dia 180 nm	244	(Alizadeh and Paydar, 2010) [116]
Al/Ti foil	RT	4	50			(Hausöl et al., 2010) [117]
Al/$Al_{2}O_{3p}$	RT	8	50	-	-	
AA6014/AA5754	230	3	50			
Al	RT	8	50	UFG, Pancake type, Dia 210 nm	310	(Tsuji et al., 2003) [118]
Al7075	250	5	-	UFG, Pancake type, Dia 300 nm	376	
IF Steel	500	7	50	UFG, Pancake type, Dia 210 nm	870	
SS400	RT	5	-	UFG, Pancake type, Dia 110 nm	1030	
Al 1100	200	6	50	UFG, Dia 270 nm	275	(Tsuji et al., 2002) [119]
IF Steel	500	5	50	UFG, Dia 210 nm	820	

RT = room temperature, blank means no clear information available, dia is mean grain diameter, # Sequence of first layer Al/Cu/Al/Zn/Al/Ni foil/Al. In the case of two dissimilar materials such as X/Y, the layers are of the order X/Y/X (where X is material 1 and Y is material 2) except otherwise mentioned. ˆ temperature is not explicitly mentioned; however, it is likely to be RT, cross layering refers to a 90° rotation to sheets before the next pass.

It can be inferred from Table 4 that a single rolling pass typically results in a 50–60% reduction. It is important to note that the rolling speed is not included here, as it is directly proportional to the constituent materials, and is selected accordingly. However, it is important to note that the speeds are adjusted so that a 50–60% reduction can be achieved in a single pass for successful completion of ARB. The temperature showed little effect on the % reduction in a single pass; however, the grain size increases with the increase in temperature. Furthermore, the tensile strength first decreases and then increases with subsequent rolling cycles due to the restoration of work-hardened layers. An increase in

the number of rolling cycles contributes towards the attainment of ultra-fine grains (UFG) and improved tensile strength.

By looking at the observations in the preceding paragraph related to Table 4, the following explanation is developed to link the PSP. It can be inferred that the sheet threshold reduction is the prime contributor to the improved bond strength. Interestingly, it is independent of material and relies significantly on process parameters such as rolling speed and number of passes which control the proportion of exposed/fractured area, thus enabling the asperities of the workpiece materials (in case of metals) to come in contact for the formation of a metallurgical bond. In addition to the asperity contact, the process transforms the original microstructure of the constituent material. As mentioned earlier, SPD processes are mostly related to grain refinement. From Table 4, it can be observed that grain refinement typically occurs at a faster rate in the beginning, but slows down with increasing deformation due to the saturation of plastic strain at the metastable grain size. Additionally, the pancake-like grain structure is more commonly noted for ARB. It is believed that grain refinement in SPD processes is mostly attributed to the Continuous Dynamic Recrystallization (CDRX) [120], which suggests pronounced dislocations mobility rather than grain boundaries along with the formation of new grains. Here, the dislocation mobility not only results in the formation of new grains through the transformation of dislocation cells into sub-grains and ultimately fine grains, it also determines the strength/mechanical properties. It is explained that the dislocation glide is a key deformation mechanism in crystalline materials in which the increase in lattice distortion density enhances the strength. It is explained that grain boundaries serve as a barrier to dislocation movement, and this effect becomes more pronounced with grain refinement due to the requirement of larger strains as fine grains can accommodate fewer piled-up dislocations, slip across boundaries needs greater external stresses. Besides the increase in tensile strength, the increase in yield strength can be explained by Hall–Petch hardening, where the increase in strength is proportional to the inverse root of the grain size for submicron size grains and is generally achieved through rotation of the sheet to 90° before the next pass.

7. Future Perspectives and Outlook

This paper provides a comprehensive review of the RB process, which entails a thorough review of the process variants, their advantages and limitations, joint evaluation with particular emphasis on microstructural characterization, mechanical and electrical properties, corrosion behavior, process applications in different industrial sectors, and identification of the key process parameters.

RB processes are well established and are being currently used in several applications. In the hot rolling domain, advances in vacuum hot roll bonding of titanium alloy and steel or stainless steel with or without interlayers is also something that has been demonstrated and represents an active area of research in this RB variant, with the ultimate goal being the bonding of ultra-thick multi metal plates for structural applications in extreme and challenging environments. From a future manufacturing perspective, the high technology readiness level of the processes can be exploited for modern applications by combining them with emerging processes. One such applications is in the field of additive manufacturing (AM). Sheet lamination is one of the fundamental AM techniques and is currently being employed through either ultrasonic additive manufacturing (UAM) and laminated object manufacturing. RB processes can be explored as a viable solution for UAM and can offer benefits such as low-cost equipment (absence of laser) and mitigating/reducing the formation of IMCs, which are typically observed in fused dissimilar joints. Another prospective application of the RB process is functionally gradient (FG) structures. By joining multiple layers of dissimilar materials through RB processes, an FG structure is possible with requisite tailored properties. However, careful selection of process parameters is a prerequisite in the development of such structures. Another area that can be addressed in future research is the formability of roll bonded sheets. Metals joined through the RB

process must undergo forming processes to be utilized in industrial or commercial applications. Additionally, the development of disassembly techniques for dissimilar materials RB joints is an unchartered research domain. The existing conventional disassembly processes result in material waste and degradation in material for future use. The development of new disassembly techniques will improve the recyclability of RB joints.

With respect to numerical modeling, the existing models are predominantly used for the validation of the experimental results or, in the case of ARB, on the grain refinement mechanism. However, to increase the application of roll bonding processes especially for dissimilar materials, accurate process modeling of process design, optimization, and automation are essential considering the complex thermomechanical (in case of hot roll bonding) and metallurgical bonding nature. These features can be incorporated through multiscale modeling with effective sub-models to describe heat transfer, changes of metallurgical and mechanical properties, material flow, and contact conditions during the process.

Author Contributions: H.A.K.: Conceptualization, Data curation, Writing—original draft preparation, Supervision. K.A.: Methodology, Writing—original draft preparation, review. F.A.: Supervision, Formal analysis. A.H.: Formal analysis, Data curation. A.K.: Writing—analysis, review and editing. B.M.: Writing—review and editing. All authors have read and agreed to the published version of the manuscript.

Institutional Review Board Statement: Not applicable.

Conflicts of Interest: The authors declare no conflict of interest.

References

1. Cai, W.; Daehn, G.; Vivek, A.; Li, J.; Khan, H.; Mishra, R.S.; Komarasamy, M. A state-of-the-art review on solid-state metal joining. *ASME J. Manuf. Sci. Eng.* **2019**, *141*, 031012. [CrossRef]
2. Wang, K.; Khan, H.A.; Li, Z.; Lyu, S.; Li, J. Micro friction stir welding of multilayer aluminum alloy sheets. *J. Mater. Process. Technol.* **2018**, *260*, 137–145. [CrossRef]
3. Khan, H.; Li, J.; Shao, C. Analyses of friction stir riveting processes: A review. *ASME J. Manuf. Sci. Eng.* **2017**, *139*, 090801. [CrossRef]
4. Wang, K.; Li, Y.; Banu, M.; Li, J.; Guo, W.; Khan, H. Effect of interfacial preheating on welded joints during ultrasonic composite welding. *J. Mater. Process. Technol.* **2017**, *246*, 116–122. [CrossRef]
5. Göken, M.; Höppel, H.W. Tailoring Nanostructured, Graded, and Particle-Reinforced Al Laminates by Accumulative Roll Bonding. *Adv. Mater.* **2011**, *23*, 2663–2668. [CrossRef]
6. Khan, H.A.; Wang, K.; Li, J. Interfacial bonding mechanism and mechanical properties of micro friction stir blind riveting for multiple Cu/Al ultra-thin layers. *Mater. Charact.* **2018**, *141*, 32–40. [CrossRef]
7. Mansouri, H.; Eghbali, B.; Afrand, M. Producing multi-layer composite of stainless steel/aluminum/copper by accumulative roll bonding (ARB) process. *J. Manuf. Process.* **2019**, *46*, 298–303. [CrossRef]
8. Horik, L.R.V.; Pfaffenberger, R.T. Roll Welded Structure and Process. U.S. Patent No. 3453717 A, 8 July 1969.
9. Yang, W. An Investigation of Bonding Mechanism in Metal Cladding by Warm Rolling. Ph.D. Thesis, Texas A&M University, College Station, TX, USA, 2011.
10. Bay, N.; Clemensen, C.; Juelstorp, O.; Wanheim, T. Bond Strength in Cold Roll Bonding. *CIRP Ann. Manuf. Technol.* **1985**, *34*, 221–224. [CrossRef]
11. Li, L.; Nagai, K.; Yin, F. Progress in Cold Roll Bonding of Metals. *Sci. Technol. Adv. Mater.* **2008**, *9*, 023001. [CrossRef]
12. Wang, H.; Zhang, D.; Zhao, D.W. Analysis of Asymmetrical Rolling of Unbounded Clad Sheet by Slab Method Considering Vertical Shear Stress. *ISIJ Int.* **2015**, *55*, 1058–1066. [CrossRef]
13. Pan, D.; Gao, K.; Yu, J. Cold Roll Bonding of Bimetallic Sheets and Strips. *Mater. Sci. Technol.* **1989**, *5*, 934–939. [CrossRef]
14. Schmidt, H.C.; Homberg, W.; Orive, A.G.; Grundmeier, G.; Hordych, I.; Maier, H.J. Cold pressure welding of aluminum-steel blanks: Manufacturing process and electrochemical surface preparation. *AIP Conf. Proc.* **2018**, *1960*, 050007.
15. Wei, Y.; Li, H.; Sun, F.; Zou, J. The interfacial characterization and performance of Cu/Al-conductive head processed by explosion welding, cold pressure welding, and solid-liquid casting. *Metals* **2019**, *9*, 237. [CrossRef]
16. Mao, Z.; Xie, J.; Wang, A.; Wang, W.; Ma, D.; Liu, P. Effects of annealing temperature on the interfacial microstructure and bonding strength of Cu/Al clad sheets produced by twin-roll casting and rolling. *J. Mater. Process. Technol. J. Mater. Process. Technol.* **2020**, *285*, 116804. [CrossRef]

17. Jamaati, R.; Toroghinejad, M.R. Cold roll bonding bond strengths: A review. *Mater. Sci. Technol.* **2011**, *27*, 1101–1108. [CrossRef]
18. Tang, C.; Liu, Z.; Zhou, D.; Wu, S. Surface Treatment with the Cold Roll Bonding Process for an Aluminum Alloy and Mild Steel. *Strength Mater.* **2015**, *47*, 150–155. [CrossRef]
19. Groche, P.; Wohletz, S.; Mann, A.; Krech, M.; Monnerjahn, V. Conjoint Forming–Technologies for Simultaneous Forming and Joining. In *Materials Science and Engineering*; IOP Conference Series; IOP Publishing: Bristol, UK, 2016; Volume 119, p. 012025.
20. Qi, Z.; Yu, C.; Xiao, H. Microstructure and bonding properties of magnesium alloy AZ31/CP-Ti clad plates fabricated by rolling bonding. *J. Manuf. Process.* **2018**, *32*, 175–186. [CrossRef]
21. Frolov, Y.; Haranich, Y.; Bobukh, O.; Remez, O.; Voswinkel, D.; Grydin, O. Deformation of expanded steel mesh inlay inside aluminum matrix during the roll bonding. *J. Manuf. Process.* **2020**, *58*, 857–867. [CrossRef]
22. Tsuji, N.; Saito, Y.; Utsunomiya, H.; Tanigawa, S. Ultra-Fine-Grained Bulk Steel Produced by Accumulative Roll-Bonding (ARB) Process. *Scr. Mater.* **1999**, *40*, 795–800. [CrossRef]
23. Jamaati, R.; Toroghinejad, M.R. Manufacturing of High-Strength Aluminum/Alumina Composite by Accumulative Roll Bonding. *Mater. Sci. Eng. A* **2010**, *527*, 4146–4151. [CrossRef]
24. Vaidyanath, L.R.; Nicholas, M.G.; Milner, D.R. Significance of Surface Preparation in Cold Pressure Welding. *Br. Weld. J.* **1959**, *7*, 1–6.
25. Quadir, M.Z.; Wolz, A.; Hoffman, M.; Ferry, M. Influence of Processing Parameters on the Bond Toughness of Roll Bonded Aluminum Strip. *Scr. Mater.* **2008**, *58*, 959–962. [CrossRef]
26. Jamaati, R.; Toroghinejad, M.R. Investigation of the Parameters of the Cold Roll Bonding (CRB) Process. *Mater. Sci. Eng. A* **2010**, *527*, 2320–2326. [CrossRef]
27. Naseri, M.; Reihanian, M.; Borhani, E. Bonding behavior during cold roll-cladding of tri-layered Al/brass/Al composite. *J. Manuf. Process.* **2016**, *24*, 125–137. [CrossRef]
28. Cave, J.A.; Williams, J.D. The Mechanisms of Cold Pressure Welding. *J. Inst. Met.* **1973**, *101*, 203.
29. Movahedi, M.; Kokabi, A.H.; Seyed Reihani, S.M. Investigation on the Bond Strength of Al-1100/St-12 Roll Bonded Sheets, Optimization, and Characterization. *Mater. Des.* **2011**, *32*, 3143–3149. [CrossRef]
30. McEwan, K.J.B.; Milner, D.R. Pressure Welding of Dissimilar Metals. *Br. Weld. J.* **1962**, *9*, 406–420.
31. Hosseini, H.R.M.; Kokabi, A.H. Cold Roll Bonding of 5754-Aluminium Strips. *Mater. Sci. Eng. A* **2002**, *335*, 186–190. [CrossRef]
32. Manesh, H.D.; Shahabi, H.S. Effective Parameters on Bonding Strength of Roll Bonded Al/St/Al Multilayer Strips. *J. Alloys Compd.* **2010**, *476*, 292–299. [CrossRef]
33. Tsuji, N.; Toyoda, T.; Minamino, Y.; Koizumi, Y.; Yamane, T.; Komatsu, M.; Kiritani, M. Microstructural Change of Ultrafine-Grained Aluminum during High-Speed Plastic Deformation. *Mater. Sci. Eng. A* **2003**, *350*, 108–116. [CrossRef]
34. Wu, G.Q.; Li, Z.F.; Luo, G.X.; Huang, Z. The Effects of Various Finished Surfaces on Diffusion Bonding. *Modeling Simul. Mater. Sci. Eng.* **2008**, *16*, 085006. [CrossRef]
35. Sahin, M. Effect of Surface Roughness on Weldability in Aluminum Sheets Joined by Cold Pressure Welding. *Ind. Lubr. Tribol.* **2008**, *60*, 249–254. [CrossRef]
36. Cantalejos, N.A.; Cusminsky, G. Morphology of the Interface of Roll Bonded Aluminum. *J. Inst. Met.* **1972**, *100*, 20–23.
37. Mori, K. *Simulation of Materials Processing: Theory, Applications, and Models*; A.A. Balkema Publishers: Tokyo, Japan, 2001.
38. Jamaati, R.; Toroghinejad, M.R. The Role of Surface Preparation Parameters on Cold Roll Bonding of Aluminum Strips. *J. Mater. Eng. Perform.* **2011**, *20*, 191–197. [CrossRef]
39. Mahabunphachai, S.; Koç, M.; Ni, J. Pressure Welding of Thin Sheet Metals: Experimental Investigations and Analytical Modeling. *ASME J. Manuf. Sci. Eng.* **2009**, *131*, 041003. [CrossRef]
40. Mohamed, H.A.; Washbush, J. Mechanism of Solid-State Pressure Welding. *Weld. Res. Suppl.* **1975**, *9*, 302.
41. Agers, B.M.; Singer, A.R. The Mechanism of Small Tool Pressure Welding. *Br. Weld. J.* **1964**, *11*, 313.
42. Jamaati, R.; Toroghinejad, M.R. Effect of Friction, Annealing Conditions and Hardness on the Bond Strength of Al/Al Strips Produced by Cold Roll Bonding Process. *Mater. Des.* **2010**, *31*, 4508–4513. [CrossRef]
43. Buchner, M.; Buchner, B.; Buchmayr, B.; Kilian, H.; Riemelmoser, F. Investigation of Different Parameters on Roll-Bonding Quality of Aluminum and Steel Sheets. *Int. J. Mater. Form.* **2008**, *1*, 1279–1282. [CrossRef]
44. Abbasi, M.; Toroghinejad, M.R. Effects of Processing Parameters on the Bond Strength of Cu/Cu Roll-Bonded Strips. *J. Mater. Process. Technol.* **2010**, *210*, 560–563. [CrossRef]
45. Lukaschkin, N.D.; Borisow, A.P.; Erlikh, A.I. The System Analysis of Metal Forming Technique in Welding Processes. *J. Mater. Proc. Technol.* **1997**, *66*, 264–269. [CrossRef]
46. Yan, H.; Lenard, J.G. A Study of Warm and Cold Roll-Bonding of Aluminum Alloy. *Mater. Sci. Eng. A* **2004**, *385*, 419–428. [CrossRef]
47. Krzyzanowski, M.; Beynon, J.H. *Oxide Behavior in Hot Rolling: Metal Forming Science and Practice*; Lenard, J.G., Ed.; Elsevier: Oxford, UK, 2002.
48. Butlin, J.; Mackay, C.A. Experiment on the Roll-Bonding of Tin Coatings to Non-Ferrous Substrate. *Sheet Met. Ind.* **1979**, *11*, 1063–1072.
49. Luo, J.G.; Acoff, V.L. Using Cold Roll Bonding and Annealing to Process Ti/Al Multi-Layered Composites from Elemental Foils. *Mater. Sci. Eng. A* **2004**, *379*, 164–172. [CrossRef]

50. Taheri, A.K.; Majlessi, S.A. An investigation into the production of bi-and tri-layered strips by drawing through wedge-shaped dies. *J. Mater. Eng. Perf.* **1992**, *1*, 285–291. [CrossRef]

51. Marouf, B.T.; Bagheri, R.; Mahmudi, R. Effects of Number of Layers and Adhesive Ductility on Impact Behavior of Laminates. *Mater. Lett.* **2004**, *58*, 2721–2724. [CrossRef]

52. Khan, H.A.; Pei, S.; Chen, N.; Miller, S.; Li, J. Evaluation of µFSBR joint performance by process-physics based quality criteria and online monitoring algorithm. *J. Mater. Proc. Technol.* **2020**, *278*, 116508. [CrossRef]

53. Scharnweber, J.; Chekhonin, P.; Oertel, C.G.; Romberg, J.; Freudenberger, J.; Jaschinski, J.; Skrotzki, W. Microstructure, Texture, and Mechanical Properties of Laminar Metal Composites Produced by Accumulative Roll Bonding. *Adv. Eng. Mater.* **2019**, *21*, 1800210. [CrossRef]

54. Liu, B.X.; An, Q.; Yin, F.X.; Wang, S.; Chen, C.X. Interface formation and bonding mechanisms of hot-rolled stainless steel-clad plate. *J. Mater. Sci.* **2019**, *54*, 11357–11377. [CrossRef]

55. Yu, C.; Qi, Z.-C.; Yu, H.; Xu, C.; Xiao, H. Microstructural and Mechanical Properties of Hot Roll Bonded Titanium Alloy/Low Carbon Steel Plate. *J. Mater. Eng. Perform.* **2018**, *27*, 1664–1672. [CrossRef]

56. Wu, K.; Chang, H.; Maawad, E.; Gan, W.M.; Brokmeier, H.G.; Zheng, M.Y. Microstructure and Mechanical Properties of the Mg/Al Laminated Composite Fabricated by Accumulative Roll Bonding (ARB). *Mater. Sci. Eng. A* **2010**, *527*, 3073–3078. [CrossRef]

57. Hebert, R.J.; Perepezko, J.H. Deformation-Induced Synthesis and Structural Transformations of Metallic Multilayers. *Scr. Mater.* **2004**, *50*, 807–812. [CrossRef]

58. Huang, X.; Tsuji, N.; Hansen, N.; Minamino, Y. Microstructural Evolution during Accumulative Roll-Bonding of Commercial Purity Aluminum. *Mater. Sci. Eng. A* **2003**, *340*, 265–271. [CrossRef]

59. Abbasi, M.; Taheri, A.K.; Salehi, M.T. Growth Rate of Intermetallic Compounds in Al/Cu Bimetal Produced by Cold Roll Welding Process. *J. Alloys Compd.* **2001**, *319*, 233–241. [CrossRef]

60. Chaudhari, P.G.; Acoff, V.L. Titanium Aluminide Sheets Made Using Roll Bonding and Reaction Annealing. *Intermetallics* **2010**, *18*, 472–478. [CrossRef]

61. Yi, S.; Schestakow, I.; Zaefferer, S. Twinning-Related Microstructural Evolution during Hot Rolling and Subsequent Annealing of Pure Magnesium. *Mater. Sci. Eng. A* **2009**, *516*, 58–64. [CrossRef]

62. Zhang, R.G.; Acoff, V.L. Processing Sheet Materials by Accumulative Roll Bonding and Reaction Annealing from Ti/Al/Nb Elemental Foils. *Mater. Sci. Eng. A* **2007**, *463*, 67–73. [CrossRef]

63. Li, X.B.; Zu, G.Y.; Wang, P. Microstructural Development and its Effects on Mechanical Properties of Al/Cu Laminated Composite. *Trans. Nonferrous Met. Soc. China* **2015**, *25*, 36–45. [CrossRef]

64. Mungole, T.; Mansoor, B.; Ayoub, G.; Field, D.P. Bifurcation in deformation behavior of Cu and Ta by accumulative roll-bonding at high temperature. *Scr. Mater.* **2017**, *136*, 87–91. [CrossRef]

65. Chekhonin, P.; Scharnweber, J.; Scharnweber, M.; Oertel, C.G.; Hausöl, T.; Öppel, H.W.H.; Jaschinski, J.; Marr, T.; Skrotzki, W. Mechanical Properties of Aluminum Laminates Produced by Accumulative Roll Bonding. *Cryst. Res. Technol.* **2013**, *48*, 532–537. [CrossRef]

66. Borts, B.V.; Korotkova, I.M.; Lopata, O.O.; Sytin, V.I.; Tkachenko, V.I.; Vorobyov, I.O. Production of Dissimilar Metals Materials by the Method of Solid-State Joining. *Open J. Met.* **2014**, *4*, 40–47. [CrossRef]

67. Luo, Z.; Wang, G.; Xie, G. Interfacial Microstructure and Properties of a Vacuum Hot Roll-Bonded Titanium-Stainless Steel-Clad Plate with a Niobium Interlayer. *Acta Metall. Sin.* **2013**, *26*, 754–760. [CrossRef]

68. Saboktakin, M.; Razavi, G.R.; Monajati, H. The Effect of Copper Interlayer on Metallurgical Properties of Roll Bonding Titanium Clad Steel. In *International Conference on Advanced Materials Engineering*; IACSIT Press: Singapore, 2011.

69. Lauvdal, S. Experimental Studies of Cold Roll Bonded Aluminum Alloys. Master's Thesis, Institutt for Materialteknologi, Trondheim, Norway, 11 August 2011.

70. Wang, C.; Jiang, Y.; Xie, J.; Zhou, D.; Zhang, X. Interface formation and bonding mechanism of embedded aluminum-steel composite sheet during cold roll bonding. *Mater. Sci. Eng. A.* **2017**, *708*, 50–59. [CrossRef]

71. Le, H.R.; Sutcliffe, M.P.; Wang, P.Z.; Burstein, G.T. Surface oxide fracture in cold aluminum rolling. *Acta Mater.* **2004**, *52*, 911–920. [CrossRef]

72. Azimi, M.; Toroghinejad, M.R.; Shamanian, M.; Kestens, L.A. The effect of strain on the formation of an intermetallic layer in an Al-Ni laminated composite. *Metals* **2017**, *7*, 445. [CrossRef]

73. Mozaffari, A.; Hosseini, M.; Manesh, H.D. Al/Ni metal intermetallic composite produced by accumulative roll bonding and reaction annealing. *J. Alloys Compd.* **2011**, *509*, 9938–9945. [CrossRef]

74. Hong, S.T.; Weil, K.S. Niobium-clad 304L stainless steel PEMFC bipolar plate material: Tensile and bend properties. *J. Power Sources* **2007**, *168*, 408–417. [CrossRef]

75. Asim, K.; Hosford, W.F.; Pan, J.; Hong, S.T.; Weil, K.S. Mechanical Behavior and Failure Mechanism of Nb-Clad Stainless-Steel Sheets. *SAE Int. J. Mater. Manuf.* **2009**, *2*, 547–554. [CrossRef]

76. Choi, S.H.; Kim, K.H.; Oh, K.H.; Lee, D.N. Tensile deformation behavior of stainless-steel clad aluminum bilayer sheet. *Mater. Sci. Eng. A.* **1997**, *222*, 158–165. [CrossRef]

77. Matsumoto, H.; Watanabe, S.; Handa, S. Fabrication of pure Al/Mg-Li alloy clad plate and its mechanical properties. *J. Mater. Process. Technol.* **2005**, *169*, 9–15. [CrossRef]

78. Kang, G.T.; Song, J.S.; Hong, S.I. Effect of Roll Bonding Temperature on the Strength and Electrical Conductivity of an α-Brass-Clad Cu–1Cr Alloy Composite. *Phys. Met. Metallogr.* **2017**, *118*, 190–197. [CrossRef]
79. Yao, G.C.; Mei, Q.S.; Li, J.Y.; Li, C.L.; Ma, Y.; Chen, F.; Liu, M. Cu/C composites with a good combination of hardness and electrical conductivity fabricated from Cu and graphite by accumulative roll-bonding. *Mater. Des.* **2016**, *110*, 124–129. [CrossRef]
80. Naeini, M.F.; Shariat, M.H.; Eizadjou, M. On the chloride-induced pitting of ultra-fine grains 5052 aluminum alloy produced by the accumulative roll bonding process. *J. Alloys Compd.* **2011**, *509*, 4696–4700. [CrossRef]
81. Mahdi, K.; Mohsen, B.; Habib, D.M.; Mahmood, P.; Babak, H. Evaluation of corrosion properties of Al/nanosilica nanocomposite sheets produced by accumulative roll bonding (ARB) process. *J. Alloys Compd.* **2013**, *576*, 66–71.
82. Khara, S.; Choudhary, S.; Sangal, S.; Mondal, K. Corrosion-resistant Cr-coating on mild steel by powder roll bonding. *Surf. Coat. Technol.* **2016**, *296*, 203–210. [CrossRef]
83. Alil, A.; Popović, M.; Bajat, J.; Romhanji, E. Mechanical and corrosion properties of AA5083 alloy sheets produced by accumulative roll bonding (ARB) and conventional cold rolling (CR). *Mater. Corros.* **2018**, *69*, 858–869. [CrossRef]
84. Wright, P.K.; Snow, D.A.; Tay, C.K. Interfacial conditions and bond strength in cold pressure welding by rolling. *Met. Technol.* **1978**, *5*, 24–31. [CrossRef]
85. Das, M.P.; Nafari, N. Adhesive Forces at Bimetallic Interfaces. *Solid State Commun.* **1986**, *63*, 367–370. [CrossRef]
86. Yu, H.; Lu, C.; Tieu, A.K.; Godbole, A.; Su, L.; Sun, Y.; Liu, M.; Tang, D.; Kong, C. Fabrication of Ultra-Thin Nanostructured Bimetallic Foils by Accumulative Roll Bonding and Asymmetric Rolling. *Sci. Rep. UK* **2013**, *3*, 2373. [CrossRef] [PubMed]
87. Fratini, L.; Merklein, M.; Boehm, W.; Campanella, D. Modeling Aspects in Accumulative Roll Bonding Process by Explicit Finite Element Analysis. *Key Eng. Mater.* **2013**, *549*, 452–459. [CrossRef]
88. Yong, J.; Dashu, P.; Dong, L.; Luoxing, L. Analysis of Clad Sheet Bonding by Cold Rolling. *J. Mater. Proc. Technol.* **2000**, *105*, 32–37. [CrossRef]
89. Pan, S.C.; Huang, M.N.; Tzou, G.Y.; Syu, S.W. Analysis of Asymmetrical Cold and Hot Bond Rolling of Unbounded Clad Sheet under Constant Shear Friction. *J. Mater. Process. Technol.* **2006**, *177*, 114–120. [CrossRef]
90. Hwang, Y.M.; Tzou, G.Y. An Analytical Approach to Asymmetrical Cold and Hot Rolling of Clad Sheet using the Slab Method. *J. Mater. Process. Technol.* **1996**, *62*, 249–259. [CrossRef]
91. Chaudhari, G.P.; Acoff, V. Cold Roll Bonding of Multi-Layered Bi-Metal Laminate Composites. *Compos. Sci. Technol.* **2009**, *69*, 1667–1675. [CrossRef]
92. Herrmann, J.; Suttner, S.; Merklein, M. Experimental investigation and numerical modeling of the bond shear strength of multi-layered 6000 series aluminum alloys. *Procedia Eng.* **2017**, *183*, 283–290. [CrossRef]
93. Lee, S.; Lee, D.N. Slab Analysis of Roll Bonding of Silver Clad Phosphor Bronze Sheets. *Mater. Sci. Technol.* **1990**, *7*, 1042–1050. [CrossRef]
94. Tzou, G.Y. Theoretical Study on the Cold Sandwich Sheet Rolling Considering Coulomb Friction. *J. Mater. Proc. Technol.* **2001**, *114*, 41–50. [CrossRef]
95. Tzou, G.Y.; Tieu, A.K.; Huang, M.N.; Lin, C.Y.; Wu, E.Y. Analytical Approach to the Cold and Hot Bond Rolling of Sandwich Sheet with outer Hard and Inner Soft Layers. *J. Mater. Proc. Technol.* **2002**, *125*, 664–669. [CrossRef]
96. Rezaii, A.; Shafiei, E.; Ostovan, F.; Daneshmanesh, H. Experimental & theoretical investigation of roll bonding process of multilayer strips by finite element method. *J. Manuf. Process* **2020**, *54*, 54–69.
97. Karakozov, E.S.; Vasil'ev, V.N.; Paraev, S.A. Cold Welding Aluminum and Copper Foil. Part 1. Plastic Deformation Process. *Weld. Int.* **1991**, *5*, 300–303. [CrossRef]
98. Barlow, C.Y.; Nielsen, P.; Hansen, N. Multilayer Roll Bonded Aluminum Foil: Processing, Microstructure, and Flow Stress. *Acta Mater.* **2004**, *52*, 3967–3972. [CrossRef]
99. Movahedi, M.; Madaah-Hosseini, H.R.; Kokabi, A.H. The Influence of Roll Bonding Parameters on the Bond Strength of Al-3003/Zn Soldering Sheets. *Mater. Sci. Eng. A* **2000**, *487*, 417–423. [CrossRef]
100. Peng, X.K.; Wuhrer, R.; Heness, G. Rolling Strain Effects on the Interlaminar Properties of Roll Bonded Copper/Aluminum Metal Laminates. *J. Mater. Sci.* **2000**, *35*, 4357–4363. [CrossRef]
101. Peng, X.K.; Wuhrer, R.; Heness, G. On the Interface Development and Fracture Behavior of Roll Bonded Copper/Aluminum Metal Laminates. *J. Mater. Sci.* **1999**, *34*, 2029–2038. [CrossRef]
102. Saito, Y.; Utsunomiya, H.; Tsuji, N.; Sakai, T. Novel Ultra-High Straining Process for Bulk Materials—Development of the Accumulative Roll-Bonding (ARB) Process. *Acta Mater.* **1999**, *47*, 579–583. [CrossRef]
103. Saito, Y.; Tsuji, N.; Utsunomiya, H.; Sakai, T.; Hong, R.G. Ultra-Fine-Grained Bulk Aluminum Produced by Accumulative Roll-Bonding (ARB) Process. *Scr. Mater.* **1998**, *39*, 1221–1227. [CrossRef]
104. Ohsaki, S.; Kato, S.; Tsuji, N.; Ohkubo, T.; Hono, K. Bulk Mechanical Alloying of Cu–Ag and Cu/Zr Two-Phase Microstructures by Accumulative Roll-Bonding Process. *Acta Mater.* **2007**, *55*, 2885–2895. [CrossRef]
105. You, C.; Xie, W.; Miao, S.; Liang, T.; Zeng, L.; Zhang, X.; Wang, H. High strength, high electrical conductivity, and thermally stable bulk Cu/Ag nanolayered composites prepared by cross accumulative roll bonding. *Mater. Des.* **2021**, *200*, 109455. [CrossRef]
106. Eivani, A.; Shojaei, A.; Salehi, M.; Jafarian, H.; Park, N. On the evolution of microstructure and fracture behavior of multilayered copper sheet fabricated by accumulative roll bonding. *J. Mater. Res. Technol.* **2020**, *10*, 291–305. [CrossRef]
107. Shayan, M.; Eghbali, B.; Niroumand, B. The role of accumulative roll bonding after stir casting process to fabricate high-strength and nanostructured AA2024-(SiO$_2$ + TiO$_2$) hybrid nanocomposite. *J. Alloys Compd.* **2020**, *845*, 156281. [CrossRef]

108. Zheng, H.; Wu, R.; Hou, L.; Zhang, J.; Zhang, M. Mathematical analysis and its experimental comparisons for the accumulative roll bonding (ARB) process with different superimposed layers. *J. Magnes. Alloys* **2020**. [CrossRef]

109. Jafarian, H.R.; Mahdavian, M.M.; Shams, S.A.; Eivani, A.R. Microstructure analysis and observation of peculiar mechanical properties of Al/Cu/Zn/Ni multi-layered composite produced by Accumulative-Roll-Bonding (ARB). *Mater. Sci. Eng. A.* **2020**, *805*, 140556. [CrossRef]

110. Zhu, Y.; Li, Z.; Xiao, Z.; Qiu, W.; Fang, M.; Chen, Z. Effect of accumulative roll-bonding process on phase transformation and magnetic properties of polycrystalline cobalt. *Mater. Charact.* **2020**, *163*, 110290. [CrossRef]

111. Rodríguez-Espinoza, B.L.; García-Pastor, F.A.; Martínez-Poveda, B.; Quesada, A.R.; Lopez-Crespo, P. High-strength low-modulus biocompatible Nb-1Zr alloy processed by accumulative roll bonding. *Mater. Sci. Eng. A.* **2020**, *797*, 140226. [CrossRef]

112. Lee, S.H.; Lee, S.R. Fabrication and Mechanical Properties of a Nanostructured Complex Aluminum Alloy by Three-Layer Stack Accumulative Roll-Bonding. *Arch. Metall. Mater.* **2015**, *60*, 1195–1198. [CrossRef]

113. Ma, M.; Huo, P.; Liu, W.C.; Wang, G.J.; Wang, D.M. Microstructure and mechanical properties of Al/Ti/Al laminated composites prepared by roll bonding. *Mater. Sci. Eng. A.* **2015**, *636*, 301–310. [CrossRef]

114. Liu, H.S.; Zhang, B.; Zhang, G.P. Microstructures and mechanical properties of Al/Mg alloy multilayered composites produced by accumulative roll bonding. *J. Mater. Sci Technol.* **2011**, *27*, 15–21. [CrossRef]

115. Schmidt, C.W.; Knieke, C.; Maier, V.; Höppel, H.W.; Peukert, W.; Göken, M. Accelerated grain refinement during accumulative roll bonding by nanoparticle reinforcement. *Scr. Mater.* **2011**, *64*, 245–248. [CrossRef]

116. Alizadeh, M.; Paydar, M.H. Fabrication of nanostructured Al/SiCP composite by accumulative roll-bonding (ARB) process. *J. Alloys Compd.* **2010**, *492*, 231–235. [CrossRef]

117. Hausöl, T.; Maier, V.; Schmidt, C.W.; Winkler, M.; Höppel, H.W.; Göken, M. Tailoring materials properties by accumulative roll bonding. *Adv. Eng. Mater.* **2010**, *12*, 740–746. [CrossRef]

118. Tsuji, N.; Saito, Y.; Lee, S.H.; Minamino, Y. ARB (Accumulative Roll-Bonding) and other new techniques to produce bulk ultrafine-grained materials. *Adv. Eng. Mater.* **2003**, *5*, 338–344. [CrossRef]

119. Tsuji, N.; Ito, Y.; Saito, Y.; Minamino, Y. Strength and ductility of ultrafine-grained aluminum and iron produced by ARB and annealing. *Scr. Mater.* **2002**, *47*, 893–899. [CrossRef]

120. Hebesberger, T.; Stüwe, H.P.; Vorhauer, A.; Wetscher, F.; Pippan, R. Structure of Cu deformed by high pressure torsion. *Acta Mater.* **2005**, *53*, 393–402. [CrossRef]